Kiefner

U.S. Department of Transportation (USDOT) Pipeline and Hazardous Materials Safety Administration (PHMSA)
Final Report No. 26-30994-600754R-Task 4

Changes to Integrity Management Reinspection Intervals for Pipelines in Hydrogen Service

Zahra Lotfian, PhD, PE, and Michiel P. Brongers, PE
June 2, 2026

INTENTIONALLY BLANK

Final Report No. 26-30994-600754R-Task 4

Final Report

Changes to Integrity Management Reinspection Intervals for Pipelines in Hydrogen Service

to

U.S. Department of Transportation (USDOT) Pipeline and Hazardous Materials Safety Administration (PHMSA)

on

June 2, 2026

Prepared by

Zahra Lotfian
Senior Engineer II

Michiel P. Brongers, PE
Principal Engineer

Approved by

Dyke Hicks
Director of Operations

Kiefner and Associates
6185 Huntley Rd, Suite J
Columbus, OH 43229

Disclaimer

This document presents findings and/or recommendations based on engineering services performed by employees of Kiefner and Associates, Inc. The work addressed herein has been performed according to the authors' knowledge, information, and belief, in accordance with commonly accepted procedures consistent with applicable standards of practice, and is not a guarantee or warranty, either expressed or implied.

The analysis and conclusions provided in this report are for the sole use and benefit of the Client. No information or representations contained herein are for the use or benefit of any party other than the party contracting with Kiefner. The scope of use of the information presented herein is limited to the facts as presented and examined, as outlined within the body of this document. No additional representations are made as to matters not specifically addressed within this report. Any additional facts or circumstances in existence but not described or considered within this report may change the analysis, outcomes, and representations made in this report.

Executive Summary

This Task 4 report was developed by Kiefner and Associates, Inc. (Kiefner) for the U.S. Department of Transportation (USDOT) Pipeline and Hazardous Materials Safety Administration (PHMSA) as part of the research project "Changes to Integrity Management Reinspection Intervals for Pipelines in Hydrogen Service" under Contract 693JK32310011POTA. The objective of the work was to evaluate how hydrogen service, including hydrogen-blended natural gas service, may affect remaining life (RL) predictions and, consequently, integrity management (IM) reinspection intervals (RI) relative to conventional natural gas service.

The assessment focused on crack-like features in the pipe body and welds, including longitudinal, circumferential, and off-axis flaws, as well as mechanical damage such as dents. Since hydrogen accelerates fatigue crack growth and reduces fracture resistance, flaw populations that might be slow-growing or benign in natural gas service can become more concerning in hydrogen service. Consequently, this study assessed RL across a range of flaw sizes, fracture toughness values, pipe geometries, and pressure cycle severities, including flaw sizes near or below the practical detection limits of in-line inspection (ILI) and non-destructive examination (NDE) tools.

Fracture mechanics-based fatigue analysis in hydrogen was performed using advanced fatigue models that capture crack growth behavior across the full fatigue spectrum, including the threshold, stable growth, and rapid growth regions. Crack growth was predicted using the Harter T-method, implemented in AFGROW software, together with fatigue crack growth rate (FCGR) data generated by Sandia National Laboratories (SNL) in hydrogen environments. By using experimentally measured FCGR data, rather than relying solely on upper-bound design curves, the analysis reduced conservatism and provided a more realistic estimate of RL in hydrogen service. Results were also benchmarked against the fatigue design curves formalized in ASME B31.12 Code Case 220. Case studies were performed assuming 100% hydrogen, as experimental results indicated that even small hydrogen concentrations can have detrimental effects on material properties, including FCGR and fracture toughness.

Hydrogen-induced cracking can occur with or without applied stress. However, crack growth rate data for hydrogen-induced cracking (HIC) are not well documented, and thus, time-dependent life calculations cannot be performed. This report focuses on hydrogen-accelerated fatigue as hydrogen FCGR data is available and can be used directly in fracture mechanics analyses to quantify RL and RIs. For the purposes of this study, a fatigue-based framework provided a practical and technically defensible basis for comparing hydrogen service with conventional natural gas (NG) service.

Across the cases studied, fatigue life in hydrogen gas was approximately one order of magnitude lower than in air, and this trend held across different pipe geometries and pressure cycle severities. For longitudinal crack-like flaws, long fatigue lives in hydrogen service were predicted under mild pressure cycling for small flaw sizes representative of flaws that may remain undetected by ILI or NDE. For such cases, conservative upper-bound design curves remain adequate for screening; based on the current results, use of ASME B31.12 upper-bound curves appears sufficient. For larger flaws (with depth greater than 40% of the pipe wall thickness (WT)), the use of actual FCGR test data predicts longer life; in some cases, approximately double that predicted by the upper-bound design curves. Under aggressive pressure cycling, the results in hydrogen service indicated that the integrity assessment of larger flaws benefits from using more realistic FCGR inputs than using the ASME B31.12 upper-bound curves.

The sensitivity studies also showed that fatigue life in hydrogen service is strongly affected by flaw depth, pressure cycle severity, and WT. Pipes with thinner WT consistently exhibited shorter fatigue life because of the smaller remaining ligament for a given normalized flaw depth. More severe pressure cycles produced shorter remaining life. Larger-diameter, thicker-wall pipes having the same outside diameter (OD)/WT ratio showed approximately twice the life, or more, for larger flaw sizes. Most longitudinal flaw failures in hydrogen service occurred only after the crack became effectively through-wall, representing a leak-before-break scenario. This is favorable from an IM standpoint because it allows a greater opportunity for detection and intervention before rupture.

Fracture toughness effects in hydrogen service were also evaluated. Reducing plane strain fracture toughness from the experimentally hydrogen tested base-case average value of 90 ksi√in to the ASME B31.12 minimum of 50 ksi√in produced only a minor reduction in fatigue life for many longitudinal flaw cases. However, further reductions in toughness, below 50 ksi√in, led to much shorter remaining life, demonstrating that very low-toughness conditions in hydrogen service remain a significant concern, particularly in vintage materials and weld regions.

Girth welds in hydrogen service introduce additional sensitivity to flaw size, weld residual stress, and geometric stress concentrations, such as hi/lo. The combined effects of higher-strength pipe grade, residual stress, and weld misalignment were shown to reduce RL. These findings indicated that girth welds should receive greater attention in hydrogen service, particularly in high-grade pipe segments, non-post weld heat-treated (non-PWHT) welds, locations with known fit-up challenges, and areas subject to higher cyclic pressure fluctuations.

The study also confirmed that dents require more conservative assessment in hydrogen service. Dents, gouges, and wrinkles can promote crack initiation during formation, fatigue cracking under cyclic loading, and reduced failure pressure in hydrogen-embrittlement materials. Hydrogen further increases failure susceptibility by reducing the plastic deformation required for crack initiation and increasing the severity of crack driving forces at dented locations. As a result, dents that may have been considered non-injurious in natural gas service may require re-evaluation and, in some cases, more advanced assessment methods and higher safety factors (SFs) for pipelines in hydrogen gas service.

From the work in this study, the following future studies are recommended to reduce uncertainty and better support implementation within IM programs for pipelines in hydrogen service:

- Probabilistic fatigue assessment: To explicitly account for uncertainty in flaw size, probability of detection (POD), probability of identification (POI), ILI/NDE sizing error, fracture toughness, FCGR scatter, residual stress, and pressure history.
- Hard spots in hydrogen and hydrogen-blended service: To quantify the relationship among local hardness, microstructure, through-wall extent, fracture resistance, and hydrogen-assisted crack initiation/growth.
- Hydrogen concentration: To quantify the effect of low and intermediate hydrogen (1% to 20%) concentrations in blended-gas service on FCGR, including the roles of hydrogen partial pressure, mixed-gas composition, and possible impurities, and to develop engineering crack-growth models for hydrogen blends rather than assuming only 100% hydrogen conditions.[1,2]
- Low-cycle fatigue: To include low-cycle fatigue associated with relatively infrequent but high-severity transient events, including start-ups, shutdowns, station recycling, blowdowns, and other non-steady operating events.

List of Acronyms and Abbreviations

AFGROW	Crack Growth Analysis Framework (originally developed by the US Air Force)
AMPP	Association for Materials Protection and Prevention
API	American Petroleum Institute
ASME	American Society of Mechanical Engineers
BM	Base Metal
CP	Cathodic Protection
CSCC	Circumferential Stress Corrosion Cracking
CVN	Charpy V-notch
ΔK	Stress-Intensity Factor Range
ΔP	Applied Pressure Range
ECA	Engineering Critical Assessment
ERW	Electric Resistance Weld
FAD	Failure Assessment Diagram
FCGR	Fatigue Crack Growth Rate
FEA	Finite Element Analysis
H_2	Hydrogen (molecule)
HAZ	Heat-Affected Zone
HIC	Hydrogen-Induced Cracking
ILI	In-Line Inspection
IM	Integrity Management
IMP	Integrity Management Program
IPC	International Pipeline Conference
Kiefner	Kiefner and Associates, Inc.
MAOP	Maximum Allowable Operating Pressure
MFL	Magnetic Flux Leakage
MOP	Maximum Operating Pressure
NDE	Non-Destructive Examination
NG	Natural Gas
OD	Outside Diameter
PHMSA	Pipeline and Hazardous Materials Safety Administration
POD	Probability of Detection
POI	Probability of Identification
PRCI	Pipeline Research Council International
PVP	Pressure Vessel and Piping
PWHT	Post-Weld Heat Treatment
QA/QC	Quality Assurance/Quality Control
RI	Reinspection Interval
RL	Remaining Life
SCC	Stress Corrosion Cracking
SCF	Stress Concentration Factor
SF	Safety Factor
SOHIC	Stress-Oriented Hydrogen-Induced Cracking
S-N	Stress-Life
SNL	Sandia National Laboratories

SMYS	Specified Minimum Yield Strength
SP	Shape Parameter
SSI	Spectrum Severity Indicator
SSWC	Selective Seam Weld Corrosion
USDOT	U.S. Department of Transportation
UTS	Ultimate Tensile Strength
WFZ	Weld Fusion Zone
WM	Weld Metal
WPS	Welding Procedure Specification
WT	Wall Thickness

Table of Contents

List of Figures

Table of Tables

1 INTRODUCTION

This Task 4 report was prepared by Kiefner and Associates, Inc. (Kiefner) as part of the research project titled "Changes to Integrity Management Reinspection Intervals for Pipelines in Hydrogen Service" for the U.S. Department of Transportation (USDOT) Pipeline and Hazardous Materials Safety Administration (PHMSA) under Contract 693JK32310011POTA.

The purpose of this task was to evaluate how integrity management (IM) reinspection interval (RI) procedures may need to be modified when pipelines operate in hydrogen or hydrogen-blended natural gas service rather than conventional natural gas service. Because different threat categories do not respond to hydrogen exposure in the same manner, this report focuses on those feature types for which hydrogen is most likely to alter remaining life (RL) and, consequently, RI determinations.

This study emphasized crack-like features[i] in the pipe body and welds, including longitudinal, circumferential, and off-axis flaws, and considered the implications of hydrogen service for mechanical damage, particularly dents. RL was defined as the time between the feature's identification and reaching critical size. RIs were then established by applying an appropriate safety factor (SF) to the calculated RL, recognizing that the selected factor depends on confidence in the assessment method, input uncertainties, and the consequences of failure.

To support these evaluations, this report applied fracture mechanics-based fatigue crack growth analysis using advanced models that represent crack growth across all growth regions (threshold, stable, and rapid), while accounting for loading ratio (R-ratio) effects. The analyses incorporate experimental fatigue crack growth rate (FCGR) data obtained in hydrogen environments to reduce unnecessary conservatism relative to traditional upper-bound design curves. Sensitivity studies were conducted to quantify the effects of flaw size, fracture toughness, pipe geometry, pressure cycle severity, and weld-specific factors, including residual stress and misalignment.

Hydrogen-induced cracking (HIC) can occur with or without applied stress. At present, crack growth rate data for HICs are not well documented, and thus, time-dependent life calculations cannot be performed. However, hydrogen-accelerated FCGRs are available. Accordingly, the focus on fatigue in this report should not be interpreted as excluding other hydrogen-assisted cracking mechanisms. Rather, fatigue behavior was selected as hydrogen FCGR data is available and can be used directly in fracture mechanics analyses to quantify RL and RIs. Given the objective of this study, to evaluate the effect of hydrogen on service life and reassessment intervals, a fatigue-based framework provided a practical and defensible basis for comparing hydrogen service with conventional natural gas (NG) service.

Table 1 summarizes the parameters investigated in this study and identifies the corresponding sections of the report in which they are presented.

[i] Unless otherwise specified, the terms flaw, feature, imperfection, and indication are used interchangeably throughout this report. In this context, the term refers to a feature detected by an inspection method. Table 5 from the Task 6 report provides details on each of these terms.

Table 1. Key Parameters Investigated for RI

Property	Section Reference for Discussion
Flaw Sizes	3.1, 3.2, 4.1, 4.3, 5.1
Flaw Location in Base Metal or weld	3.5, 5.3
FCGR	2.4, 3.3, 5.3.1.1
Fracture Toughness	3.4, 4.2, 5.3.3
Pipe Grade	3.4, 5.3.1
Pipe OD/WT	3.5, 3.7, 4.1
Hydrogen Partial Pressure (% of Hydrogen)	3.5
Cyclic Pressure	3.8, 4.1, 5.1, 5.3.1

2 BACKGROUND

2.1 General

The global shift towards hydrogen as a clean energy source has brought significant attention to pipeline mechanical integrity. Hydrogen's unique properties, such as its propensity to embrittle pipeline materials, accelerate FCGRs and reduce fracture toughness, pose safety and reliability challenges that conventional analysis methods cannot adequately address. These issues are further compounded by the industry's move to blend hydrogen with natural gas. The concern is that subcritical flaws that would be considered benign in natural gas may grow and become critical over time, threatening infrastructure when pipelines are exposed to hydrogen gas.

While pressure cycle fatigue may not typically be a significant concern in conventional gas pipelines, introducing hydrogen changes the dynamic. Hydrogen embrittlement accelerates crack growth and reduces material toughness, making pressure-cycle fatigue analysis a critical component of mechanical integrity assessments. As the industry shifts towards hydrogen blending in natural gas pipelines, accurate RL assessments under fatigue conditions become essential for effective IM.

As part of ongoing research for PHMSA, this report addresses the challenge of assessing the RL of various types of flaws residing in the steel of hydrogen and blended hydrogen-natural gas pipelines. The RL of these flaws was estimated through a series of case studies, accounting for variables such as flaw size, fracture toughness, pipe geometry, and the severity of pressure cycles. Advanced fatigue models were employed to capture crack growth across Regions I (threshold), II (stable growth), and III (rapid growth), integrating experimental FCGR data to reduce conservatism relative to traditional upper-bound design curves.

2.2 Reinspection Intervals

Theoretically, a pipeline's life can be infinite, provided the asset is adequately maintained. However, pipeline integrity is threatened by various causes that must be managed to ensure safe operations. Codes, such as ASME B31.8S-2018,[3] list specific integrity threats, usually associated with the pipe's physical features and metallurgical conditions. Integrity management programs

(IMPs) rely on in-line inspection (ILI), non-destructive examination (NDE), or other methods to find those features.

Once the feature locations are detected, their identity is positively established, their current dimensions are known, and a likely future growth rate is known; their anticipated RL can be estimated, and appropriate responses can be executed. These activities must be done on a schedule, with reinspection/reassessment before the feature becomes critical. Thus, to avoid failure, the RI should be set to a value shorter than RL (e.g., half of RL).

Operators should evaluate all detected features and estimate their individual RLs. The feature with the shortest life will be the "weakest link" that dominates the entire pipeline's life. The operator should repair or remove/cut out all features with an RL shorter than the desired RI.

In addition to the parameters mentioned above, the following is a non-exhaustive list of factors that should be considered in the RL determination:

- Basic pipeline design, steel properties, and operational details - through data integration;
- Diameter, wall thickness (WT), specified minimum yield strength (SMYS), ultimate tensile strength (UTS), and assumptions on material properties;
- Seam weld type, vintage, coating type, and cathodic protection (CP) or no CP;
- Maximum allowable operating pressure (MAOP), pressure fluctuations, temperature, known history, threat identification, and threat interactions;
- Properties of the features;
- Characteristics at time of inspection (probability of detection (POD), identification, sizing);
- Estimated growth rates;
- Assumptions on growth mechanism;
- Assumptions on rate with time (constant or changing rate);
- Properties of critical size features;
- Definition of failure (depth-through-wall percentage, flow strength, fracture toughness);
- Uncertainty in all parameters;
- Decision on RI; and
- The length of the desired interval.

The process of establishing an RI is illustrated in Figures 1 through 5. The period of interest is operations, which can last many decades. Periodic maintenance should be planned, and operators typically have a system to ensure these standard activities are accomplished. If maintenance is performed such that anomalies never reach critical dimensions, the pipeline's life can be infinite, as illustrated in Figure 1.

Features other than pipe manufacturing defects initiate sometime after the pipeline is placed into service. For example, it takes time for a coating to disbond and for corrosion-induced metal loss to occur on the metal surface. From the moment a feature initiates, it can grow at a rate determined by the growth mechanism and environmental and operational conditions. Failure is usually defined as the point at which a feature reaches a critical size, leading to pipe leakage or rupture. Thus, the total feature life from initiation to a critical size is shown in Figure 2.

Features cannot be identified at the time of initiation, as they are too small. Sometime later, during the feature's subcritical life, it can be detected by an inspection. The time between the moment that a feature is detected/identified and the time that it grows to critical size is the RL of the feature, as shown in Figure 3.

The RI should be set well before a feature becomes critical. A typical value engineers use is a Factor 2, signifying the RI should not exceed half of the RL; refer to Figure 4. However, the SF depends on various parameters, including confidence in the methodology used to estimate the RL and the consequences of failure.

For a collection of features, such as the entire collection of anomalies detected in an ILI run, the shortest RL of a feature dominates and limits the pipeline's RL. The desired RI can be reached by repairing/removing those features with the shortest RL. The non-repaired features should be monitored until the next inspection/assessment; refer to Figure 5.

THE REMAINDER OF THIS PAGE IS INTENTIONALLY BLANK

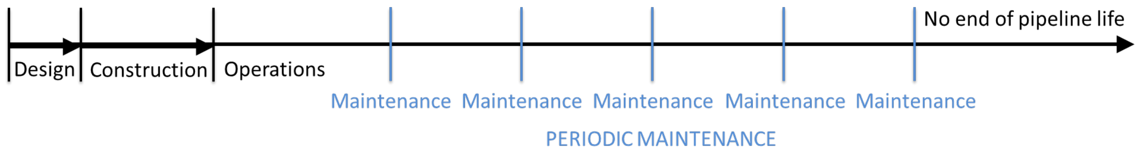

Figure 1. Timeline Showing Periodic Maintenance at Regular Intervals During Pipeline Operation

Figure 2. Timeline Showing Feature Life from the Time of First Initiation with Feature Growth Until the Feature's Critical Size is Reached

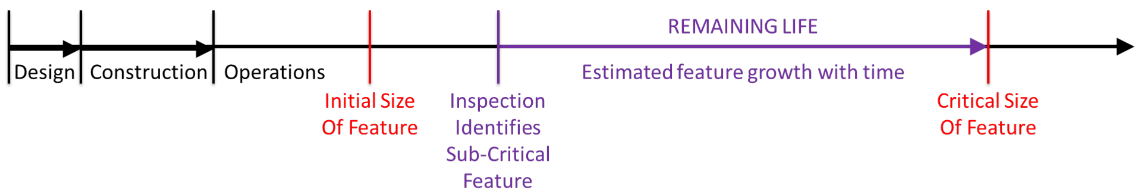

Figure 3. Timeline Showing RL is Shorter Than the Total Feature Life

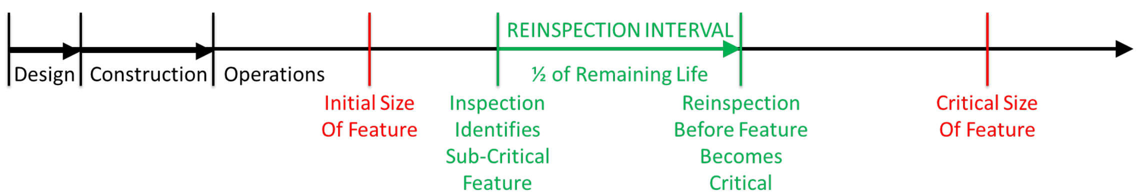

Figure 4. Timeline Showing an RI of a Single Feature as Half of the Feature's RL

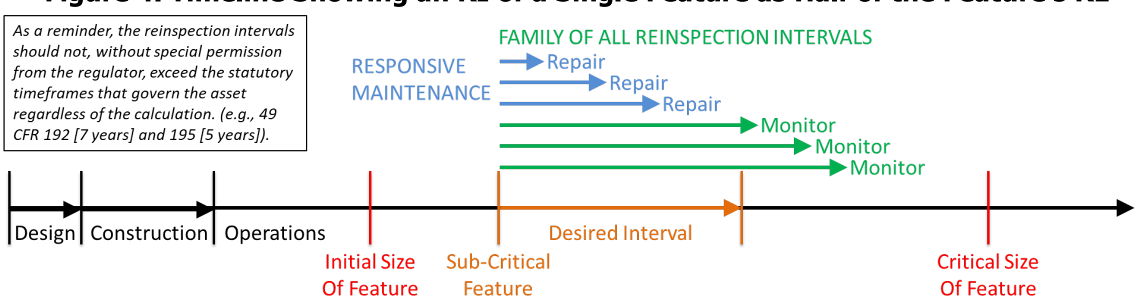

Figure 5. Timeline Showing that the Desired (Reinspection) Interval of a Collection of Features is Determined by the Shortest RL of Any Single Feature that is Not Repaired

2.3 Overview of Fatigue Remaining Life Analysis

The fatigue process generally progresses through three stages: crack initiation, crack propagation, and final failure. Each stage is influenced by a range of factors, as discussed in a BMT report[4].

Broadly, fatigue damage accumulation is governed by three primary categories: loading conditions, material properties, and structural/feature geometry.

Loading Factors:

- Cycle magnitude;
- R-ratio;
- Cycle frequency;
- Load sequence (order of cycles); and
- Number of load cycles.

Material Factors:

- FCGR, i.e., da/dN behavior;
- Base metal (BM) vs. weld metal (WM) properties;
- Material grade and vintage; and
- Environmental conditions.

Geometric Factors:

- Pipe outside diameter (OD) & WT;
- Flaw dimensions (length, depth) and location; and
- Weld misalignment and weld geometry.

In practice, all three categories must be considered to achieve adequate fatigue performance. While some factors may have a more dominant influence, extreme values in any category can lead to significantly reduced fatigue life.

2.3.1 Fatigue Crack Initiation Phase

The fatigue crack initiation phase encompasses the formation and early development of small crack-like features in components that are initially free of detectable defects. Crack initiation typically occurs at the microstructural level at locations that act as local strain concentrators. These include inclusions, second-phase particles, porosity, and microvoids.

Even in nominally defect-free materials, crack initiation is strongly influenced by macroscopic stress concentrators arising from geometric and fabrication features. Such locations include notches, weld toes, pre-existing weld imperfections, and regions with abrupt thickness changes. These features elevate local stresses and strains, thereby accelerating the initiation process.

The duration of the initiation phase can vary significantly depending on material properties, surface condition, and loading severity. Under high-stress or low-cycle fatigue conditions, crack initiation may occur rapidly, whereas at lower stress amplitudes, it may account for a substantial portion of the total fatigue life.

For components without pre-existing crack-like defects, fatigue behavior in this phase is commonly characterized using stress-life (S-N) curves, which relate cyclic stress amplitude to the number of cycles required for crack initiation.

2.3.2 Fatigue Crack Propagation Phase

Once a distinct crack is present in a structure, whether initiated by the mechanisms described above or pre-existing damage (e.g., environmental cracking or weld imperfections), it will propagate incrementally with each applied load cycle. Under cyclic loading, the crack propagates until the remaining ligament can no longer withstand the applied stresses, leading to final failure.

When a discrete crack exists, fatigue behavior is no longer adequately described by S-N methods. Instead, fracture mechanics-based approaches are required to explicitly model crack growth on a cycle-by-cycle basis. These methods relate the FCGR to the applied stress-intensity factor range (ΔK) and the effective loading ratio (R-ratio), enabling the prediction of crack propagation and RL under specified loading conditions.

2.4 Overview of Fracture Mechanics-Based Fatigue Analysis for H_2 Pipelines

Fracture mechanics is the study of the propagation of cracks in materials. Fracture mechanics-based fatigue approaches provide a more rigorous and physically representative framework, particularly for cases involving pre-existing crack-like features. These methods quantitatively relate the crack size, the structural and local geometry, the material properties, and explicitly model crack growth using relationships between FCGR (da/dN) and ΔK. However, they are more complex and require detailed inputs, including initial flaw size, stress intensity calculations, material crack growth data in hydrogen environments, and sometimes finite element analysis (FEA).

The following sections provide a brief overview of fracture-mechanics-based assessment approaches for addressing challenges in hydrogen- and hydrogen-natural gas-blended pipelines. More detailed discussions of the inputs and their effects on the integrity assessment results for these pipelines are presented in subsequent sections of this report.

The steel's fatigue response is characterized by three regions, generally referred to as Region I (threshold), Region II (stable crack growth), and Region III (rapid crack growth); see Figure 6. Most pipeline fatigue analyses focus on Region II, characterized by a power-law relationship between the FCGR (da/dN). This is the change in crack depth, a, per cycle, N, and ΔK. This relationship is the Paris equation. A limitation of the Paris equation is that the FCGR in Region I is modeled unrealistically fast, and in Region III, unrealistically slow.

Paris Equation:

$$\frac{da}{dN} = C\,(\Delta K)^n \quad (1)$$

Where:

da = the change in crack size

dN = the incremental load cycle

da/dN = the crack size increase per applied load cycle

ΔK = the change in applied stress intensity factor (i.e., the crack driving force)

C and n = crack growth rate constants (curve-fitting parameters)

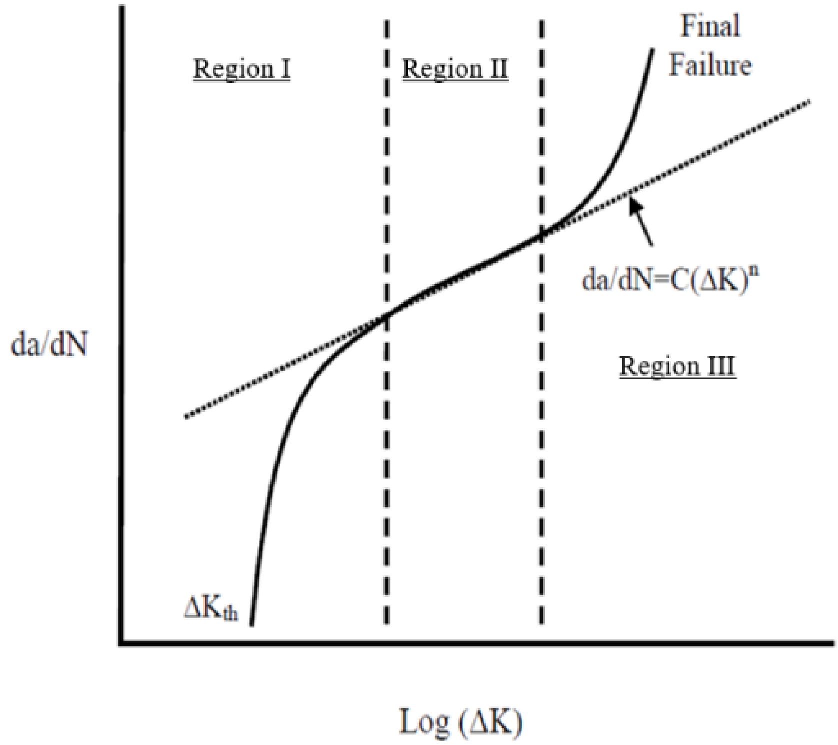

Figure 6. Fatigue Crack Growth Rate in Different ΔK Regions

With the introduction of hydrogen into existing pipelines and the emerging need for pipeline crack-growth management, this study considers a more advanced crack-growth analysis. It represents the full spectrum of behavior across the low, medium, and high ΔK regions. The Walker equation modifies the Paris equation by introducing a parameter (m) that adjusts the magnitude of data shifting as a function of the minimum-to-maximum load ratio (R-ratio) in the cycle. This is important because laboratory test data are often limited to a few R-ratios. The Walker equation allows adjustment without requiring retesting at many different R-ratios.

Walker Equation

$$\frac{da}{dN} = C\left(\Delta K(1-R)^{(m-1)}\right)^n \tag{2}$$

$$R = \frac{K_{min}}{K_{max}} \tag{3}$$

Where:

m = the stress shift parameter

ΔK used in the Paris equation represents the crack driving force and is a function of the crack size and shape, the structural geometry being considered, and the applied loading (i.e., internal pressure range). It is calculated using the following general equation:

$$\Delta K = Y\,(\Delta\sigma)\sqrt{\pi a} \quad (4)$$

Where:

Y = geometry factor associated with both the crack and structural geometry

$\Delta\sigma$ = applied pipe wall stress range

a = crack size (depth)

There are several approaches to calculating the geometry factor (Y) used in stress intensity factor calculations. For simplified generic structural and crack geometries subjected to simplified loading, a few compendia provide equations for calculating Y, including API 579 and BS 7910. For more complicated structural geometries or loading scenarios, detailed FEA techniques can also be used to estimate the geometry factor (Y).

2.4.1 Crack Growth Rate Calculations

The simplified iterative process used in carrying out a fracture mechanics-based fatigue life assessment of a pipeline containing a crack is summarized below.

1. Calculate ΔK for the initial surface flaw size (i.e., the initial depth, a_i and length $2c_i$) and the applied pressure range (ΔP).
2. Calculate the amount of crack extension (Δa and Δc) that occurs for the Nth cycle of ΔP using the finite form of the Paris equation.
3. Calculate the new crack size based on the current size and the amount of crack extension.

$$a_{i+1} + 1 = a_i + \mathrm{D}a \quad (5)$$

$$2c_{i+1} = 2c_i + 2\mathrm{D}c \quad (6)$$

4. Calculate the new stress intensity factor range (ΔK_{i+1}) based on the updated crack size and the applied pressure range.
5. Repeat Steps 2 through 4 until the final flaw size (a_f and $2c_f$) is reached.

3 INPUTS TO FATIGUE MODEL

Case studies were performed considering various pipeline conditions, including flaw size, fracture toughness (also called fracture resistance), and pressure cycle severity. Hill et al.[5] and Schroeder et al.[6] conducted a sensitivity study of hydrogen's effects on pipeline integrity.

3.1 Initial Flaw Size

Each operator is responsible for determining the types and sizes of features that exist or are likely to exist in their system. ASME B31.12[7] does not specify initial flaw sizes for fatigue analysis of hydrogen or hydrogen-natural gas blended pipelines. The initial flaw size used as the starting point for a fracture mechanics-based fatigue life assessment can be estimated using a variety of methods, including:

- Crack detection ILI tools or in-field NDE techniques;

- Historical manufacturing workmanship acceptance criteria associated with typical line pipe; and
- Estimate based on the family of the largest defects that could survive a pressure test (either actual or proposed).

The PHMSA Task 6 Report[8] of the present study provides a detailed description of each of the above methods and available tools. Table 2 provides examples of typical features and their detectable minimum sizes using different ILI techniques based on data provided by Novitech, Inc.[9] for their Micron magnetic flux leakage (MFL) and Deformation ILI tools.

Table 2. Summary of Detectable Feature Sizes for the Micron ILI Novitech Tools

Feature Type	ILI Technique	Detectable Minimum Size	Probability of Detection
Metal Loss (General, Pitting, Axial Grooving, Circumferential Grooving)	Axial MFL	10% of WT	95%
Metal Loss (Pinholes, Axial Slotting, Circumferential Slotting)	Axial MFL	20% or 10% of WT[ii]	95%
Crack-like (Narrow Axial)	Circumferential and Axial MFL + IDD-SM	20% of WT	>90%
Crack-like (Narrow Circumferential)	Circumferential and Axial MFL + IDD-SM	25% of WT	>90%
Deformations	Geometry Tool	The greater of 0.5% OD or 0.030 inches	>99%

Since the detectable flaw size ranges vary between vendors, can be dependent upon ILI run quality, and may even vary between different tools from the same vendor, the present study analyzed a range of practical depths and lengths for undetected features to ensure comprehensive coverage, as shown in Table 3. Initial flaw depth (a_0) values are expressed as a percentage of the WT. As discussed next, the effect of pipe grade on fracture toughness has already been accounted for. Therefore, the analysis focused solely on API 5L[10] Grade X52 linepipe steel for the case studies.

[ii] Minimum detectable size is dependent upon the width and length of the metal loss found; further details are in the source documentation.

Table 3. Input Parameter Values Used in Sensitivity Studies

Property	Base Case Value	Range of Tested Values
Flaw Depth, a_0/WT	60%	5%, 10%, 15%, 20%, 40%, 60%, 80%
Flaw Length	3 in	0.5, 1.0, 1.5, 2.0, 3.0 in
Pipe OD/WT	10 /0.25 (in/in)	10/0.25, 20/0.50 (in/in)
Fracture Toughness (Plane Strain/Plane Stress)	90/176 (ksi√in)	90/176, 50/98, 40/78, 30/59, 25/49, 20/39 (ksi√in)
Maximum Operating Pressure (MOP) and Spectrum Severity Indicator (SSI)	50% SMYS, 25	50% SMYS/25, 72% SMYS/75, 72% SMYS/147

3.2 Critical Flaw Size

In this study, cracks were modeled to propagate until they reached the critical crack size, beyond which further growth becomes unstable, leading to rapid crack extension. At that point, the pipe was considered to have failed. The critical crack size was defined as the flaw dimensions for which the applied stress intensity factor, $K_{applied}$, from the pressure-induced hoop stress equaled the material's fracture toughness, K_{mat}. When $K_{applied} \geq K_{mat}$, failure is predicted. This condition can occur in two scenarios:

- Before the critical crack depth, a, reaches 80%[iii] of the WT (a_{crit} < 80% of the WT). This scenario could occur for materials with low toughness or very long cracks in more ductile steels.
- After the crack depth becomes through-wall. This scenario is more favorable, as it represents a leak-before-break condition, allowing for potential detection and mitigation before catastrophic (rupture) failure.

Additionally, a failure assessment diagram (FAD)-based approach can be used to transition to a through-wall crack, employing methods described in API 579-1/ASME FFS-1-2021[11], such as CorLAS™.[12] A few cases were studied using the FAD approach to critical flaw size.

The analysis begins with an initial crack size and progresses iteratively until the critical crack size is reached. ΔK for each cycle increment is calculated for the flaw's length and depth directions based on its current size and the pipeline loading conditions. Using an FCGR curve, the crack advancement rates in the length and depth directions are determined from the corresponding ΔK values, with the specific R-ratio for that cycle taken into account. The crack depth and length are then updated individually. After each update, the critical condition is evaluated. If the critical crack size is reached, the crack growth loop terminates.

[iii] 80% WT is the threshold typically used to assume a through-wall crack.

3.3 Experimental FCGR Data

ASME B31.12 Code Case 220[13] formalizes fatigue design curves for gaseous hydrogen that account for the loading R-ratio, ΔK, and the hydrogen gas pressure, g(P), as a function of overall pressure, P.

In this study, experimental FCGR test data measured in laboratory-scale experiments with hydrogen environments were used to reduce conservatism in the analysis by replacing standard fatigue design curves, such as those in ASME B31.12[7], with empirical data. This approach provides a more accurate representation of crack growth within the specific data range considered. This study used FCGR test data in hydrogen from Sandia National Laboratories (SNL), which was developed as part of the HyBlend project.[6]

These data were also included in the AFMAT fracture mechanics database[14], which is integrated into the AFGROW software tool[15] for fatigue crack growth analysis that was used in this study. Originally developed by the Air Force Research Laboratory and now maintained by LexTech, Inc., AFGROW is widely used for fatigue analysis in the aerospace and nuclear industries. It incorporates the Harter T-method[16,17] to determine FCGR for different R-ratios from just a few ΔK-da/dN curves. This is a very important advantage of this method, because the data on FCGRs are relatively limited, as they address only a few loading R-ratios.

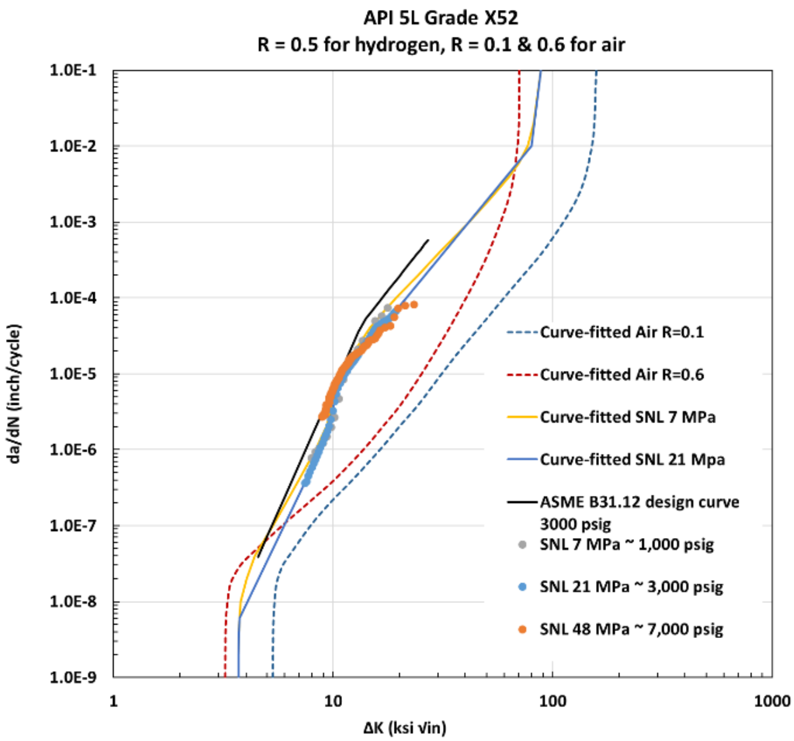

Figure 7. FCGR Curves for API 5L Grade X52 Line Pipe Steel Samples Tested in Hydrogen and in Air, Based on Data from SNL and ASME B31.12 Design Curve

Figure 7 shows an example of the SNL data for an API 5L Grade X52 linepipe steel tested in the BM in a 100% hydrogen gas environment at R = 0.5 under three different hydrogen pressures. The data at 7 MPa (1,000 psig) and 21 MPa (3,000 psig) are particularly relevant to the range of interest for pipelines repurposed for hydrogen service. Due to challenges in collecting experimental test data at the extreme lower and upper thresholds, the SNL data primarily covers Region II. This study's data has been curve-fitted based on the SNL 21 MPa[iv] base-metal data to extend coverage into these threshold regions. The value, m, in the Walker equation is determined using the Harter T-method from these experimental test data.

The experimental test results show minimal variation and negligible differences when extended to line pipe steel Grades X42 and X60. Similar FCGR data for air at R = 0.1 and R = 0.6 are also plotted for comparison. When comparing the FCGRs in hydrogen with those in air, it is evident that, for typical ΔK values, the air curves exhibit significantly lower FCGRs than the hydrogen curves. However, at the limiting edges, the hydrogen-charged data appear to converge with the air FCGR data in Regions I and III (for the same R-ratio).

3.4 Fracture Toughness and Pipe Grade

Material strength (grade) and fracture toughness (fracture resistance) are correlated, and, in general, steels exhibit greater susceptibility to hydrogen embrittlement with higher material strength. Studies[18,19,20] show that the Mode I threshold stress intensity factor in hydrogen, K_{IH}, decreases as yield strength increases, as shown in Figure 8. Based on the tests conducted by Ronevich et al.[20], the average fracture resistance under plane-strain conditions was approximately 100 MPa√m (91 ksi√in) for line pipe Grades X42 and X52, and approximately 80 MPa√m (73 ksi√in) for Grade X60.

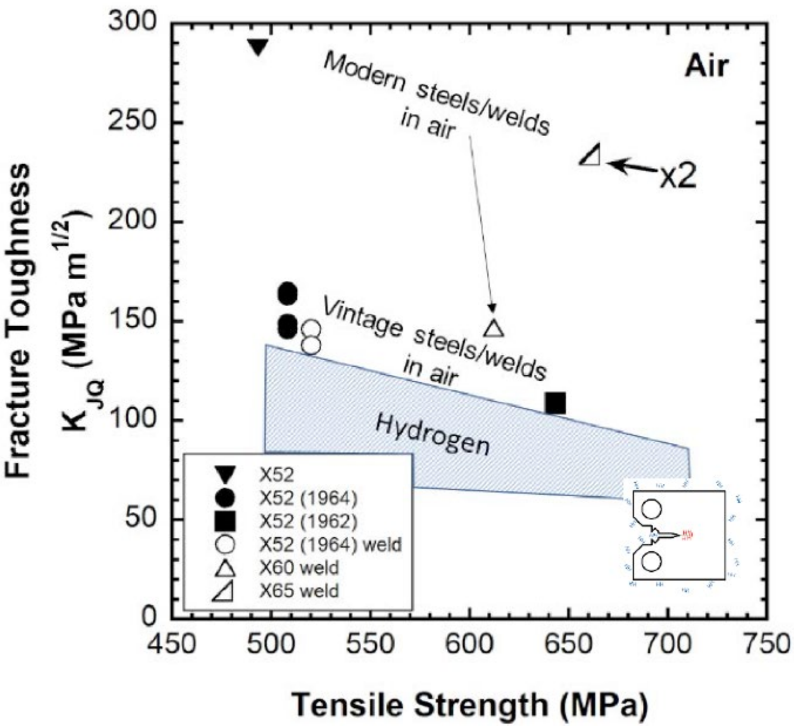

Figure 8. Fracture Toughness in Air and in Hydrogen as a Function of Yield Studies[20]

[iv] The 21 MPa BM data were selected for this study because the SNL database contains only weld fusion zone (WFZ) and heat-affected zone (HAZ) data at this pressure. This enables future studies to explore the effects of BM versus WFZ and HAZ.

The maximum applied stress intensity factor, K_{IA}, can be calculated for given flaw dimensions at design pressure. For the flaw to survive, K_{IH} shall be equal to or higher than the calculated value of K_{IA}. In any case, ASME B31.12-2023 requires that the K_{IH} of a material shall not be less than 55 MPa√m (50 ksi√in).

Considering these findings, two ranges of plane strain fracture toughness (K_C) were selected for the primary evaluation: a minimum of 50 ksi√in and an average of 90 ksi√in. Corresponding plane stress fracture toughness (K_{IC}) values were proportionally set at 98 ksi√in (minimum) and 176 ksi√in (average). Other lower fracture toughness values were also analyzed to observe the fatigue-life trend in very low-toughness conditions.

Plane-stress and plane-strain fracture toughness values are material properties. However, in this study, the apparent fracture toughness was used to define the stress intensity failure limit. The apparent fracture toughness value was determined by a linear interpolation between the plane-strain and plane-stress fracture toughness based on the thickness and applied stress. The highest possible value of apparent fracture toughness is the plane-stress fracture toughness, and the lowest possible value is the plane-strain fracture toughness. The apparent toughness and stress state are typically between the plane-stress and plane-strain modes.

3.5 Hydrogen Partial Pressure (% of Hydrogen)

Experimental studies[21,22] have shown that the FCGR and fracture toughness of API pipeline steels can be significantly affected by hydrogen, even at relatively low hydrogen concentrations (1%) and at partial pressures as low as 0.1 MPa.

Regarding fracture toughness, gaseous hydrogen mixtures have been shown to exhibit a substantial effect. As illustrated in the bar chart in Figure 9, the difference between 1% hydrogen and 100% hydrogen is relatively modest, indicating that even low hydrogen concentrations can meaningfully reduce fracture resistance.

At high crack-driving force (i.e., high ΔK), the FCGR becomes largely insensitive to pressure and remains approximately an order of magnitude greater than in air, even at hydrogen partial pressures as low as 0.1 MPa. Under these conditions, 1% hydrogen and 100% hydrogen may produce a similar level of severity, as shown in Figure 10. However, in the intermediate ΔK region, the FCGR in 3% hydrogen is lower than that in 100% hydrogen, indicating a measurable dependence on hydrogen partial pressure. In Figure 10, the dashed lines represent the ASME B31.12 design curves used to bound fatigue crack growth behavior.

Because hydrogen can be detrimental even at relatively low concentrations, this study conservatively assumed a 100% hydrogen environment. Future studies may further examine the effect of hydrogen partial pressure, particularly in the intermediate FCGR region where concentration dependence appears to be more pronounced.

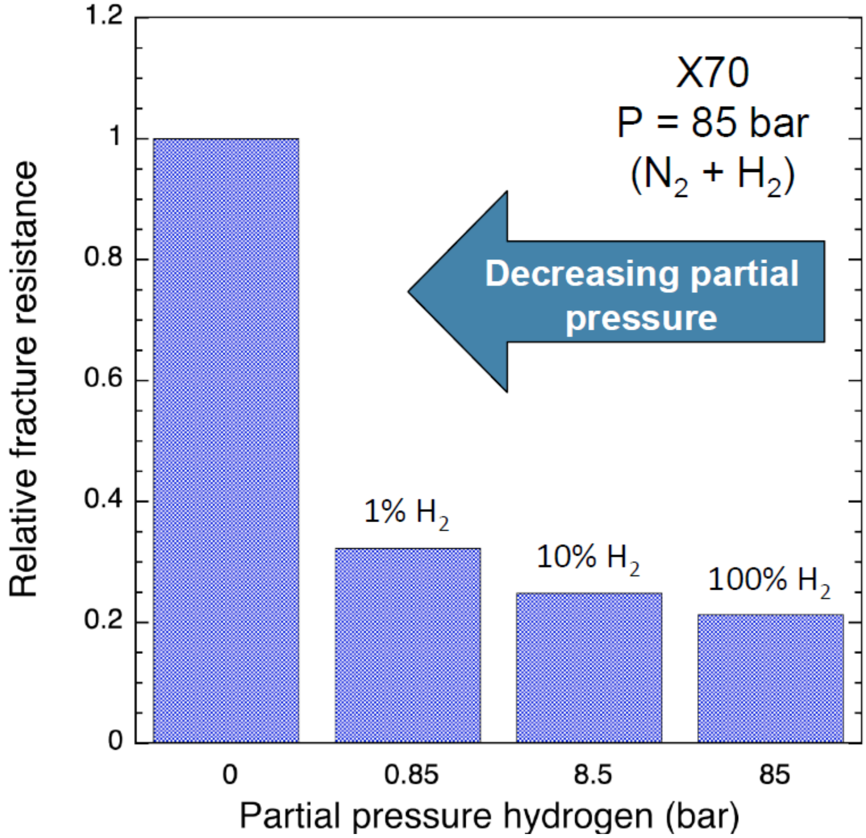

Figure 9. Effect of Hydrogen Partial Pressure on Fracture Resistance of Grade X70 Linepipe Steel at 85 Bar (1,232 psig)

THE REMAINDER OF THIS PAGE IS INTENTIONALLY BLANK

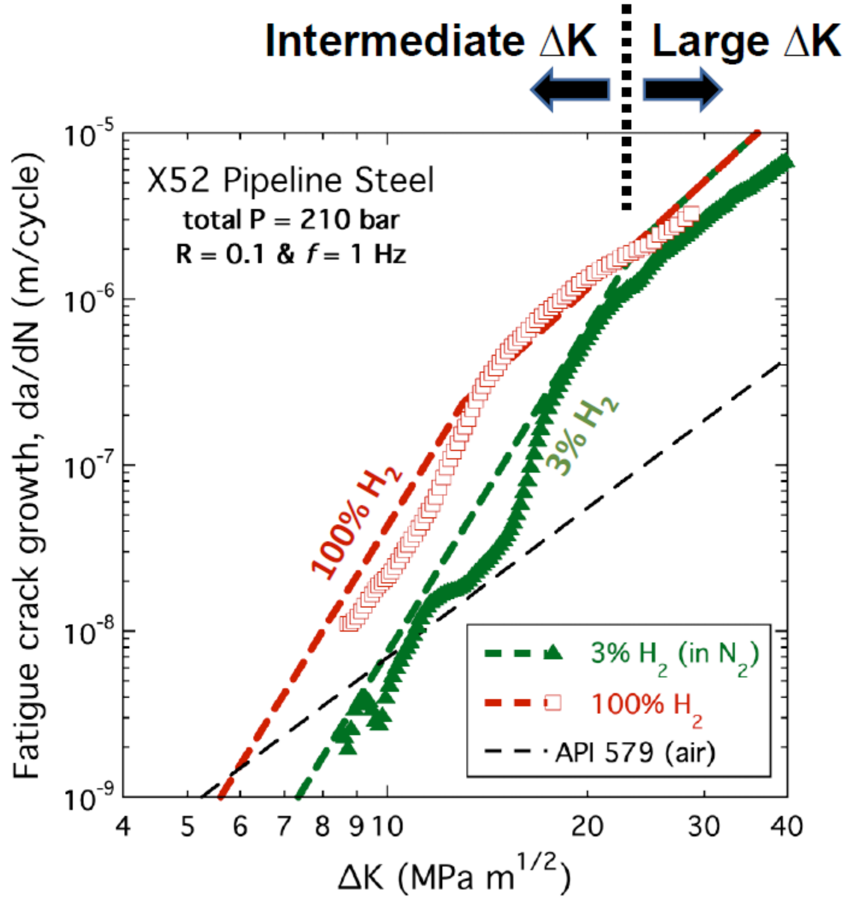

Figure 10. Fatigue Crack Growth Curves for Grade X52 Linepipe Steel at 3% and 100% Gaseous Hydrogen

3.6 Flaw Geometry and Location on Weld or BM

For the longitudinal crack-like features described in Section 4, the analysis assumed the same crack geometry specified in ASME B31.12, namely an axially oriented semi-elliptical surface flaw on the internal pipe wall. For the circumferential flaws described in Section 5, a semi-elliptical surface flaw on the internal pipe wall was similarly assumed. The corresponding stress intensity factor and reference stress solutions for these geometries were obtained using the API 579 solution procedures.

Experimental studies conducted by SNL[20,23] indicated that the WFZs and HAZs exhibit fatigue crack growth behavior in hydrogen environments comparable to that of BM, provided that residual stresses are appropriately accounted for. Similar trends have been observed across different welding processes, as illustrated in Figure 11. Accordingly, in this study, the fatigue crack growth behavior of the WFZ and HAZ was assumed to be consistent with that of the BM, with weld residual stresses explicitly included in the assessment.

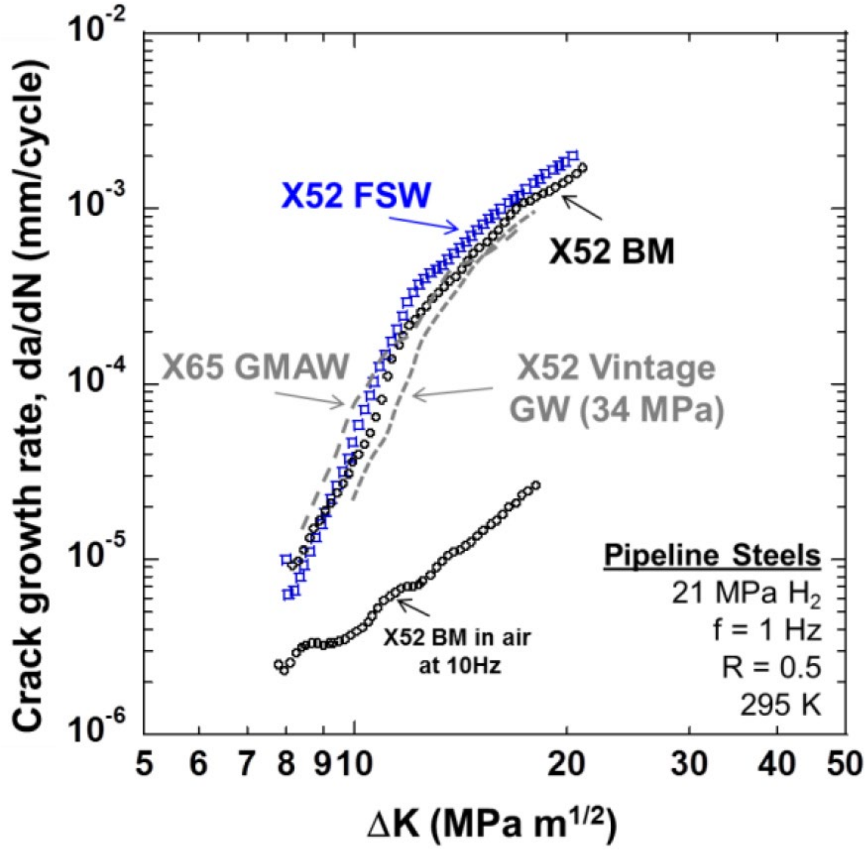

Figure 11. FCGR for Pipeline Steels Tested in Hydrogen Gas for Various Cases of BM and Welds. Included Are Data for X52 BM in Air[23]

3.7 Pipe Geometry

Two ODs of 10 and 20 inches were considered, paired with a WT of 0.25 and 0.50 inches, respectively. Both cases maintain an OD/WT ratio of 40, a typical value for transmission pipeline applications.

3.8 Pressure Cycle Severity

To evaluate the effect of internal pressure cycles, three spectra with similar trends but varying levels of severity were applied in this study. The spectrum severity indicator (SSI) quantifies the severity of cyclic fatigue associated with the pressure time history. SSI is the number of cycles of characteristic stress that results in the same fatigue damage (i.e., crack growth) as the actual pressure time history over the course of a year. The standard SSI definition is based on a hoop stress range of 13 ksi, which was used in this study. For more information on SSI, refer to the 2018 paper by Semiga et al.[24]

The first pressure spectrum used in the study had an actual maximum operating pressure (MOP) of 1,300 psig, corresponding to 50% of SMYS, and an SSI of 25, which is classified as mild cycling for a gas pipeline. The second pressure spectrum had an actual MOP of 1,872 psig, representing 72% of SMYS, with an SSI of 75, classified as moderate cycling for a gas pipeline. The third pressure spectrum had an SSI of 147, classified as aggressive cycling for a gas pipeline. The selection of these spectra, based on their MOP of 50%/72% of the SMYS, reflects the upper bound of the design pressure limits for Option A (prescriptive design) and Option B (performance-based design), respectively, as defined in ASME B31.12-2023. The analysis accounted for the characteristics of the pressure cycles, including the cycle sequence and the amplitude of individual cycles.

3.9 Various Feature Types

Several anomalies/features can reduce the fatigue life of a pipeline. The most significant of these are the crack-like features as listed below. The significance of detected crack-like features is that, as evidenced by their existence, the crack initiation portion of the fatigue life is already "used up" and only the crack propagation remains. Such crack-like features that may lead to fatigue concerns in a gas pipeline could be:

- Stress corrosion cracking (SCC);
- Weld seam defects (e.g., longitudinal electric resistance weld (ERW) faults);
- Selective seam weld corrosion (SSWC) (treated as a planar flaw);
- Girth weld and seam weld defects;
- Toe cracks, lack of fusion, undercuts, incomplete penetration, and porosity;
- Dent with gouges;
- Hard spots cracking,[25] and
- Hydrogen-induced cracking (HIC) and stress-oriented hydrogen-induced cracking (SOHIC).[v]

These features could be oriented in the longitudinal (axial), circumferential, or off-axis directions. In a fatigue analysis, these features are all considered as planar, crack-like flaws. The next section assesses the fatigue RL of each of these features, based on their orientation.

A more detailed description of different feature types that can be affected by hydrogen embrittlement was provided in the Task 3 Final Report[26] of this study.

4 FATIGUE REMAINING LIFE OF LONGITUDINAL CRACK-LIKE FEATURES

In this study, the reported fatigue life is intentionally not adjusted for SFs and is presented as calculated. A base case was analyzed, serving as the benchmark for comparing other cases. Using the base case parameters,

Figure 12 illustrates depth and length growth as a function of the number of cycles on a logarithmic scale, comparing behavior in a 100% hydrogen gas environment to that in air. The results show that the fatigue life in air is approximately one order of magnitude larger than in hydrogen gas.

[v] The high-temperature failure mechanisms of HIC, SOHIC, and hydrogen blistering are common in the chemical/petrochemical process industries but are uncommon in natural gas pipelines. Exceptions may include when the gas contains hydrogen sulfide (H_2S) and free water, when the temperature is above ambient, when the pipeline is constructed with spiral-welded pipe, and/or when the steel has laminations in its microstructure.

This trend remained consistent even when larger pipe diameters or more aggressive pressure cycles were considered.

Additionally, both the air and hydrogen cases exhibited a leak-before-break scenario. The program assumed a through-wall crack when the flaw depth reached 80% WT. However, because the applied stress intensity factor, $K_{applied}$, for the through-wall crack has not yet reached the material's fracture toughness, K_{mat}, the through-wall crack was predicted to propagate in the axial (length) direction until K_{mat} is achieved.

In a separate analysis, the effect of WT was evaluated for two pipes with the same OD/WT ratio. Figure 13 shows that, as expected, pipes with a lower WT consistently exhibited shorter fatigue lives due to the reduced remaining ligament for flaws with the same length and depth-to-WT ratio. Additionally, the figure shows that more severe pressure cycles lead to a decrease in fatigue life.

4.1 Influence of Flaw Size, Pressure Severity, and Pipe Geometry

Results for four different flaw depths (a_0) were reported: 20%, 40%, 60%, and 80% of the WT. For each depth, sensitivity analyses were conducted at five flaw lengths (inches): 0.5, 1.0, 1.5, 2.0, and 3.0, as shown in Figures 14 through 17. These plots illustrate the calculated RL in years as a function of the combination of flaw length and normalized flaw depth (a_0/wt). The RL values exceeding 100 years are grouped under the ">=100 years" category. Smaller depths and lengths were tested but resulted in significantly longer fatigue life and are not reported here, as the trend was clear.

Overall, experimental test results for pipeline steel in hydrogen gas, together with a more accurate fatigue model, showed that undetected flaws with depths less than 40% of the WT and lengths up to 3 inches on a pipeline with mild pressure cycles exhibited very long fatigue life, indicating fatigue insensitivity. For more aggressive pressure cycles, undetected flaws with depths up to 40% of the WT and lengths up to 1.5 inches showed fatigue life exceeding 100 years.

Additionally, for larger flaw sizes, cases with larger OD and WT (with the same OD/WT ratio) demonstrated fatigue lives approximately twice as long or longer. For more aggressive pressure cycles, the impact of crack depth was significant: changing the flaw depth by a factor of 2 resulted in at least a two-fold change in fatigue life. The effect of pressure cycle severity was particularly pronounced in smaller OD/WT pipes, especially for flaws with depths greater than 40% of the WT.

For illustration purposes in Figure 13, the life cycles are plotted only until the crack reaches 80% WT. Beyond this point, the crack is assumed to become through-wall and to continue growing in the longitudinal direction.

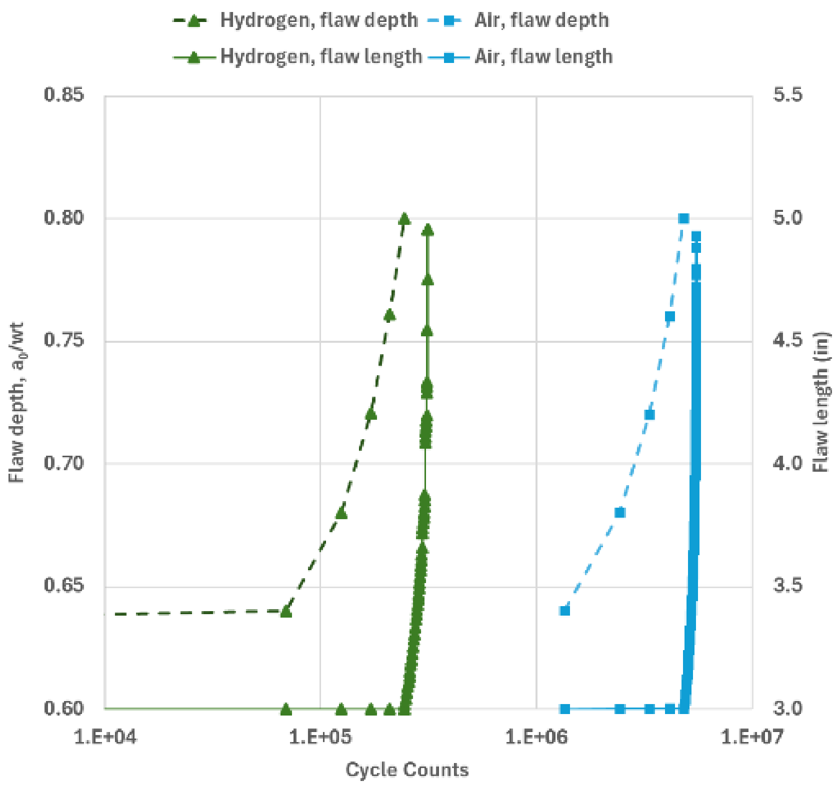

Figure 12. Normalized Flaw Depth and Length Growth vs. the Number of Cycles in Hydrogen and Air

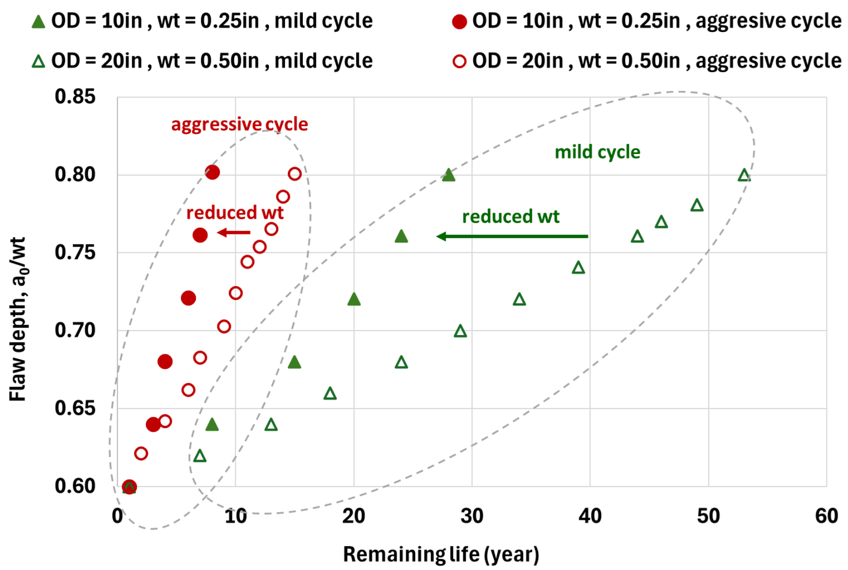

Figure 13. Normalized Flaw Depth vs. RL for Various Pressure Cycle Severity and Pipe Geometry

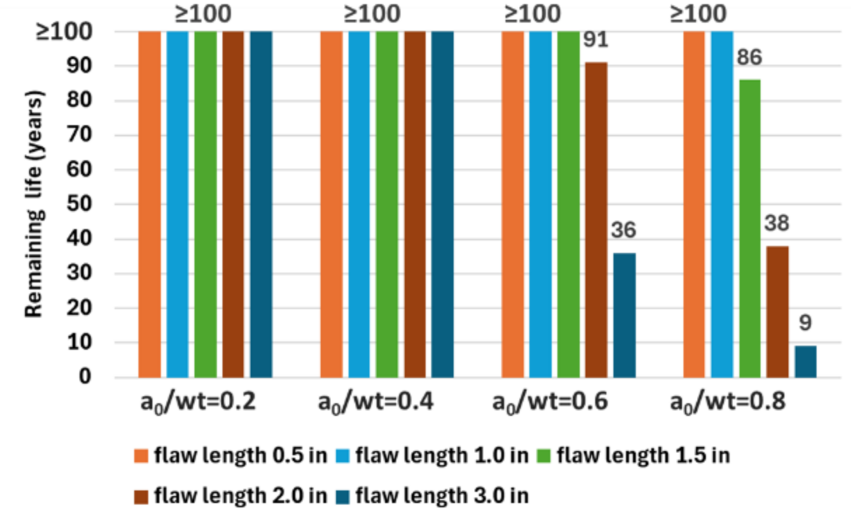

Figure 14. RL for Mild Cycles, OD = 10 in, WT = 0.25 in

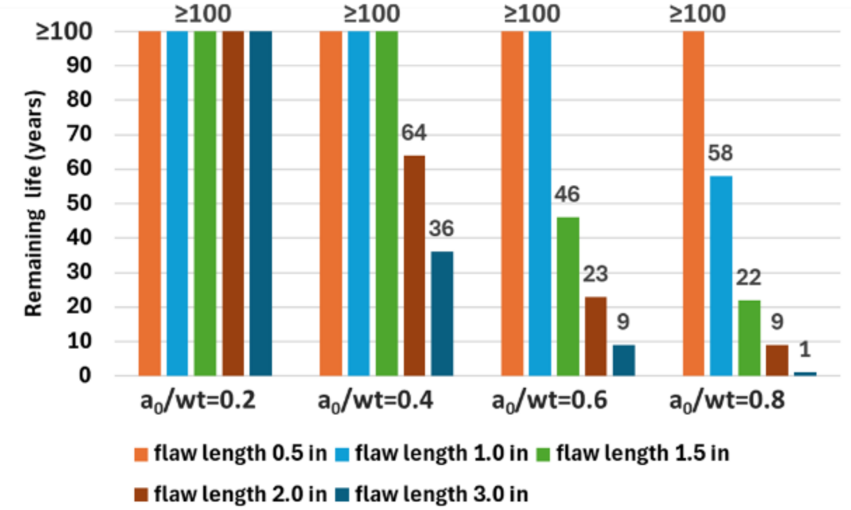

Figure 15. RL for Aggressive Cycles, OD = 10 in, WT = 0.25 in

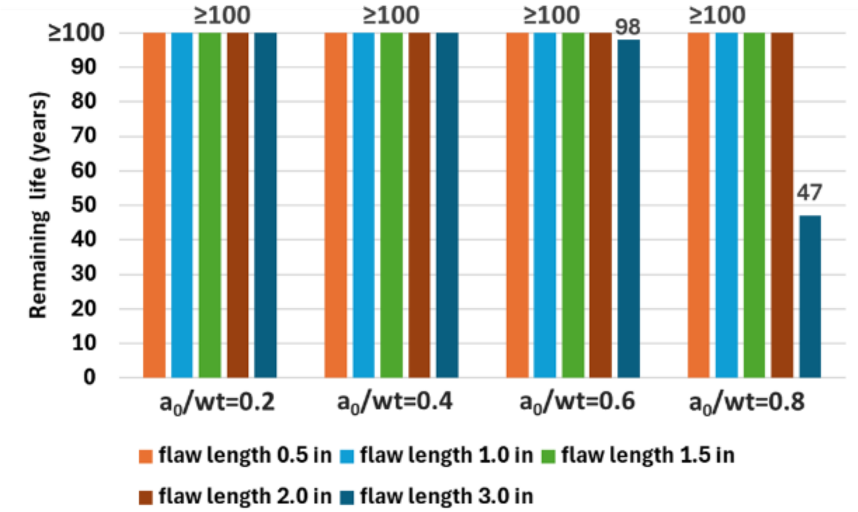

Figure 16. RL for Mild Cycles, OD = 20 in, WT = 0.50 in

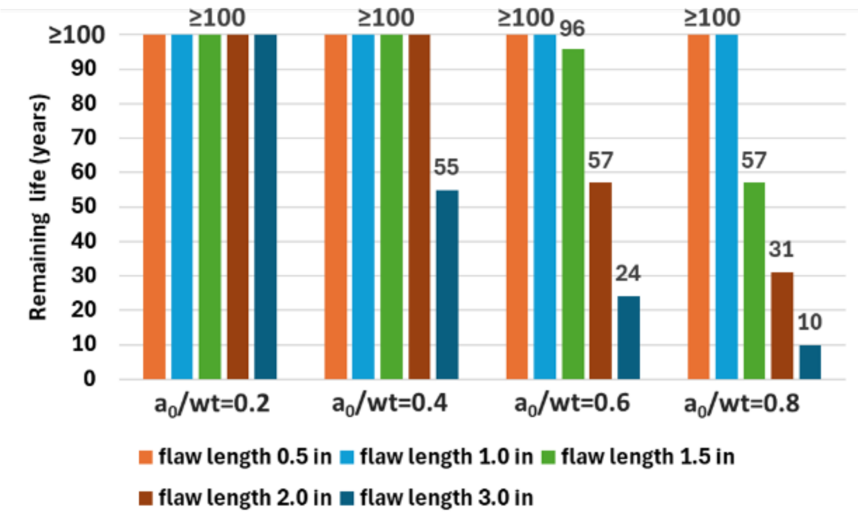

Figure 17. RL for Aggressive Cycles, OD = 20 in, WT = 0.50 in

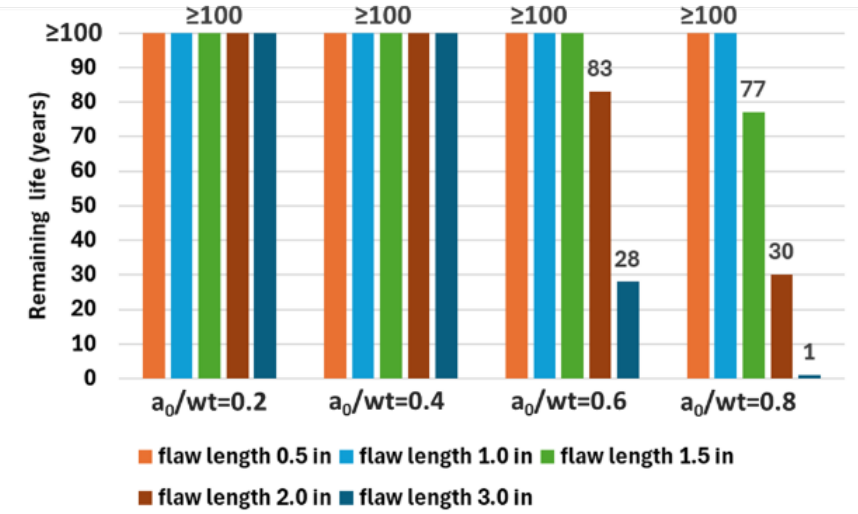

Figure 18. RL for Low-Toughness Material, Mild Cycles, OD = 10 in, WT = 0.25 in

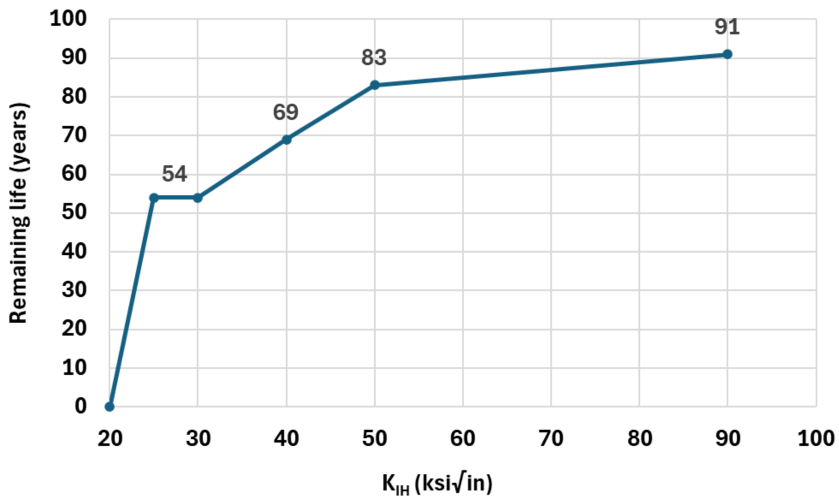

Figure 19. RL Based on K_{IH} Fracture Toughness, Mild Cycles, OD=10 in, WT = 0.25 in, a0/WT = 0.6, Flaw Length = 2.0 in

4.2 Influence of Fracture Toughness

Comparing the results in Figure 14 to those in Figure 18, shows that reducing the plane strain fracture toughness, K_{IH}, from the base case value of 90 ksi√in (and the corresponding plane stress toughness) to the minimum code requirement of 50 ksi√in results in only a slight reduction in fatigue life for flaws with depths exceeding 60% of the WT and lengths greater than 2 inches. However, further reductions in K_{IH} (and the corresponding plane-stress toughness) lead to a more significant decrease in fatigue life, as illustrated in Figure 19. Notably, when K_{IH} drops below 20 ksi√in, the feature fails immediately, with no remaining fatigue life.

4.3 Influence of Criteria for End of Fatigue Life

Changing the transition criteria for defining through-wall cracks from 80% of the WT to the CorLAS™ model had no significant impact on the RL for the base-case values in Table 3 across the different flaw sizes tested. When fracture toughness was reduced to 50 ksi√in, the fatigue life for one case showed a slight reduction, but the effect was negligible. Overall, the 80% cut-off and the CorLAS™ model yielded similar results under typical conditions. The 80% cut-off is widely accepted as a threshold to avoid errors in stress-intensity-factor calculations when the remaining ligament becomes very small, and plane-strain conditions are no longer satisfied.

Most of the fatigue life reported in this study corresponds to cases in which the crack transitions from a surface crack to a through-wall crack (reaching 80% WT is the threshold used to assume a through-wall crack), but continues to grow until it reaches the unstable growth condition ($K \geq K_{mat}$), marking the end of life. If, instead, the fatigue life is defined as ending when the crack becomes through-wall (indicating leakage), then the calculated fatigue life would be shorter. For the flaw sizes examined using the base case parameters, this difference in definition resulted in less than a 50% variation in fatigue life.

4.4 Near-neutral pH SCC – Crack and Corrosion Growth Rates

Hydrogen may be present both as gaseous hydrogen transported within the pipeline and as atomic hydrogen generated locally through corrosion reactions at the crack tip, along crack walls, and on disbonded pipe surfaces. A portion of this hydrogen diffuses into the steel and is transported to regions of high stress concentration, particularly at and near the crack tip, where it contributes to localized embrittlement.

The presence of hydrogen weakens interatomic bonds and promotes brittle crack growth. These coupled electrochemical and mechanical processes govern SCC propagation and are conceptually described by the bathtub models of Parkins.[27] However, they are inherently difficult to quantify under field/lab conditions, particularly when both internally transported gaseous hydrogen and corrosion-generated hydrogen may contribute to the overall cracking behavior.

Consistent with these mechanisms, field observations indicate that fatigue loading alone is not the dominant driver of near-neutral pH SCC growth. For example, there is a lower incidence of axial SCC failures in liquid product pipelines than in gas pipelines, despite comparable or more severe pressure cycling. This suggests that environmental and hydrogen-related factors play a more significant role than pressure-cycle severity. To date, no clear correlation has been established between SCC growth and pressure cycling metrics, further highlighting the importance of electrochemical processes that are not readily measured or predicted.

Recognizing these challenges, Pipeline Research Council International (PRCI) project MAT-8-7 proposes a data-driven framework for modeling SCC growth based on field measurements.[28,29] In this approach, the total crack growth rate is represented as a combination of corrosion-driven and mechanically driven components. The mechanical growth term is calibrated to observed data and effectively serves as a surrogate for stress/strain rate effects and other complex interactions, including hydrogen-assisted mechanisms that are not explicitly modeled. The corrosion-related component captures the environmentally driven contribution to crack growth, while the mechanical term reflects the influence of loading, including implicit rate-dependent effects.

5 FATIGUE REMAINING LIFE OF CIRCUMFERENTIAL CRACK-LIKE FEATURES

5.1 Pipe Body Features

Circumferentially oriented cracks may occur in the pipe body (e.g., circumferential SCC [CSCC]) or at girth welds. In the absence of a significant externally imposed axial load, such as that produced by ground movement (settlement, landslides, frost heave, etc.), the dominant primary stress from internal pressure produces a lower crack-driving force for circumferential cracks on the pipe body compared to the case of longitudinal cracks.

In 2013, Fessler and Batte[30] conducted a project for PRCI to review documented CSCC cases, better understand their causes, and evaluate management approaches. The results provided guidance to operators and ILI vendors for detecting, identifying, sizing, and mitigating CSCC.

A sensitivity analysis like that performed for longitudinal cracks was carried out in this study. Table 3 shows the input parameter values used in the sensitivity scenarios. The calculations were performed comparing circumferential cracks (Figure 20) against longitudinal cracks (Figure 21) under a similar scenario and the same loading condition: internal pressure only. No residual stresses, no stress concentration effects, and no ground-induced longitudinal forces were included. The results are presented for a 10-in OD, 0.25-in WT pipeline with an aggressive pressure cycle (SSI = 147).

The bar charts illustrate the calculated RL in years as a function of the combination of flaw length and normalized flaw depth (a_0/WT). The RL values exceeding 100 years are grouped under the ">=100 years" category. Comparing Figure 20 with Figure 21 shows that circumferential cracks generally exhibit much longer fatigue life than longitudinal cracks under pure pressure cycling because the effective driving stress range is substantially lower (often on the order of ~1/3 of that for comparable longitudinal cracks due to Poisson/constraint effects). This observation is consistent with the study by Lamborn et al.[31], which concluded that fatigue crack growth in circumferential and off-axis flaws due to pressure cycling is unlikely.

However, the fatigue life of circumferential cracks can be reduced by other loads and growth mechanisms, including construction loads (e.g., in field bends), thermal cycles, external loads (e.g., ground movement–induced forces), live traffic/vibration, and time-dependent crack growth processes such as those associated with CSCC.

THE REMAINDER OF THIS PAGE IS INTENTIONALLY BLANK

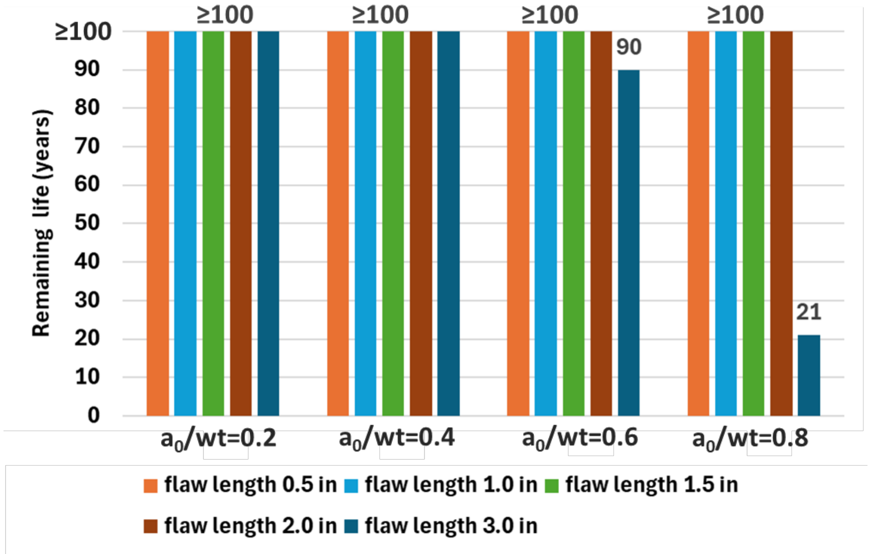

Figure 20. Remaining Fatigue Life of Circumferential Cracks in a 10-in OD, 0.25-in WT Pipeline, Under Aggressive Cycles

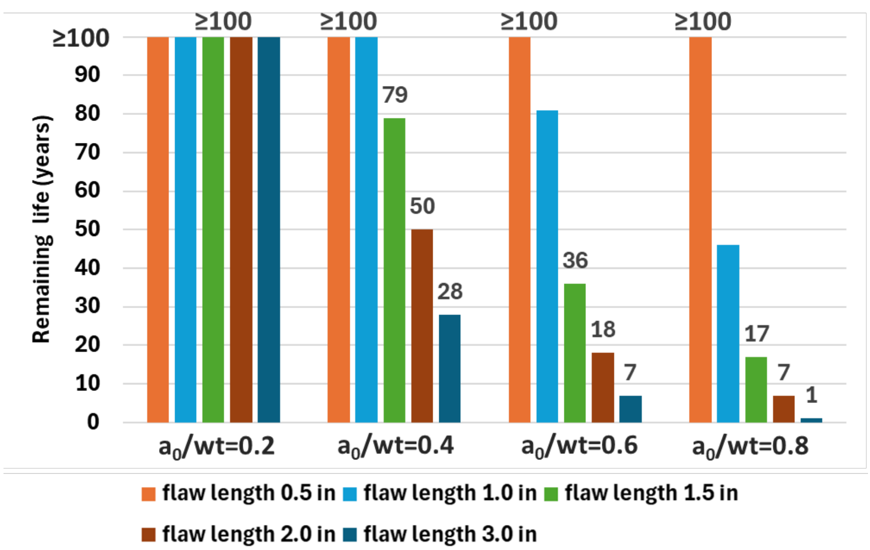

Figure 21. Remaining Fatigue Life of Longitudinal Cracks in a 10-in OD, 0.25-in WT Pipeline, Under Aggressive Cycle

5.2 Off-Axis Features

An actual ILI-detected off-axis crack-like feature by the Novitech Micron tool was assessed.[32] An equivalent flaw dimension approach based on API 579[11] was employed to calculate the equivalent dimensions in each direction. Equations (7) and (8) and Figure 22 show the calculations and the off-angle geometry for a crack-like feature.

Table 4. Data for the ILI-Detected Off-Axis Crack-Like Feature

Property	Value
Nominal OD	6.625 inch
WT	0.250
SMYS	60 ksi
Feature depth	46% WT
Feature length	0.46 inch
Feature width	2.17 inch
Off-axis orientation	154° ($\alpha = -64°$)
Depth tolerance at 80% certainty	±15% WT
Width tolerance at 80% certainty	±0.6 inch
Orientation tolerance	±10 degrees
Tool Technology	6" Micron AMFL+CMFL+ GEO+ IDD-SM

For the plane of the flaw projected on the plane normal to σ_1:

$$\frac{c}{c_m} = cos^2(\alpha) + \frac{(1-B)sin(\alpha)cos(\alpha)}{2} + B^2 sin^2(\alpha) \quad (5)$$

For the plane of the flaw projected on the plane normal to σ_2:

$$\frac{c}{c_m} = \frac{cos^2(\alpha)}{B^2} + \frac{(1-B)sin(\alpha)cos(\alpha)}{2\,B^2} + sin^2(\alpha) \quad (6)$$

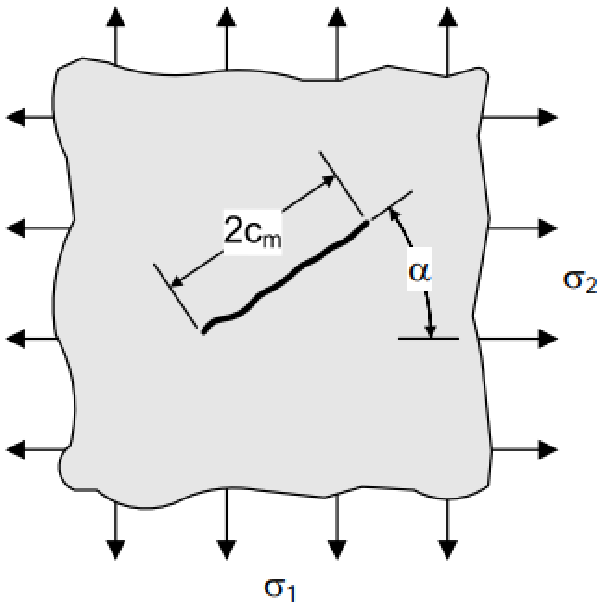

Figure 22. Schematic Showing of Off-Axis Crack-Like Feature

Assuming the worst-case scenario by adding depth, width, and orientation tolerances, the remaining fatigue life of the feature under mild, moderate, and aggressive pressure cycle regimes was estimated to exceed 100 years.

5.3 Girth Weld and Field Welds Features

Compared to circumferential flaws in the pipe body, those located in field welds (e.g., branch connections, fillet welds to fittings, or repair welds), and particularly in girth welds, exhibit distinct characteristics due to welding processes and fabrication practices:

1. Residual Stress: Girth welds introduce weld residual stresses, which can increase the crack-driving force.
2. Stress Concentration: Elevated stress concentrations are often present at welds due to misalignment (hi/lo) and other geometric discontinuities.
3. The challenge is compounded in vintage pipelines. Weld centerlines and HAZs in vintage pipelines often exhibit hardened layers, lower fracture toughness, and may contain weld-related defects (such as lack of fusion and undercut), creating a more vulnerable starting point for hydrogen-related cracking. Discussion on the weld FCGR can be found in Section 3.5.

5.3.1 Residual Stress

Residual stresses can affect fatigue behavior based on their magnitude and sign (i.e., positive or negative). Additionally, residual stresses scale with yield strength, so they are greater in higher-strength materials. Whether to include residual stress and its magnitude can affect the failure pressure and the remaining fatigue life.

One potentially significant factor that has not always been fully accounted for in weld assessments is the effect of residual stresses on FCGR behavior. Residual stresses, common in field welds due to thermal cycles during welding, can significantly increase the crack-driving force, accelerate crack growth, and, in some cases, promote localized hydrogen accumulation at the crack tip.

The influence of residual stress on fatigue behavior depends on both its magnitude and sign (i.e., positive or negative). Tensile residual stresses are particularly detrimental because they increase the effective R-ratio and ΔK, thereby leading to higher FCGRs. In general, the magnitude of residual stress scales with the material's yield strength. Therefore, higher-grade steel pipes tend to exhibit higher residual stress levels.

Several additional factors can significantly influence the magnitude and distribution of residual stress in welds. Post-weld heat treatment (PWHT), when applied, can reduce residual stresses through stress relaxation and redistribution, thereby improving fatigue performance. However, PWHT is not typically applied to most field girth welds in pipelines. This is particularly true for vintage pipeline systems.

Pipe vintage also plays a critical role. Older pipelines often exhibit greater variability in welding practices, heat input, and workmanship. This can lead to more irregular residual stress fields and, in some cases, higher residual stress levels. In addition, the absence of modern material control and inspection requirements (e.g., limited toughness characterization or inconsistent welding procedures) can further increase uncertainty in residual stress distributions.

Given these factors, the inclusion (or exclusion) of residual stresses, along with assumptions about their magnitude and distribution, can significantly affect both the predicted failure pressure and the remaining fatigue life. As such, careful consideration of residual stress is essential for realistic and defensible fatigue and engineering critical assessments (ECAs).

5.3.1.1 Residual Stress Effects on FCGR

To date, only a few studies have examined the fatigue behavior of pipeline steel welds in hydrogen. Ronevich et al.[18,33] tested WM, HAZ, and BM specimens in air and in high-pressure hydrogen gas to examine how residual stress and hydrogen environments interact. They found FCGR was consistently faster in welds than in BM, even in air, due in part to residual tensile stresses.

In hydrogen, the effect was amplified; welds with residual stress showed significant acceleration of FCGR compared to the BMl. This is because residual tensile stresses in the welds act as a mean stress, increasing the load ratio (R) at the crack tip.

$$R = \frac{K_{min}+K_{res}}{K_{max}+K_{res}} \quad (7)$$

Where:

K_{min}= the stress intensity factor at minimum load without considering weld residual stress

K_{max} = the stress intensity factor at maximum load without considering weld residual stress

K_{res} = the stress intensity factor due to weld residual stress

With a higher R, the FCGR curve effectively shifts to the left, meaning that crack growth starts at a lower ΔK than it would in a stress-free specimen. This is shown in Figure 23. Because the FCGR relationship is exponential, and because hydrogen FCGRs are typically about an order of magnitude higher than those in air, the effect of residual stress in increasing the effective R-ratio is more pronounced in hydrogen environments than in air. Accordingly, the residual stress state should be explicitly considered when calculating FCGR for weld regions in hydrogen service, as it directly affects the effective load ratio and the predicted crack growth behavior.

The following factors affect residual stress:

- Residual stress depends on the welding heat input, which is proportional to the welding current and voltage, and is inversely proportional to the travel speed.
- The linear heat input is normalized by the weldment thickness to distinguish between low, medium, and high heat input conditions, each associated with a different residual stress distribution. The distribution is shown in Figure 24. In general, lower heat input and greater thickness result in higher residual stress levels.
- The most conservative distribution corresponds to the low heat input case. This condition is physically representative of thick sections or very low heat input (and consequently multiple weld passes for a given thickness), which is not typically representative of most process equipment.

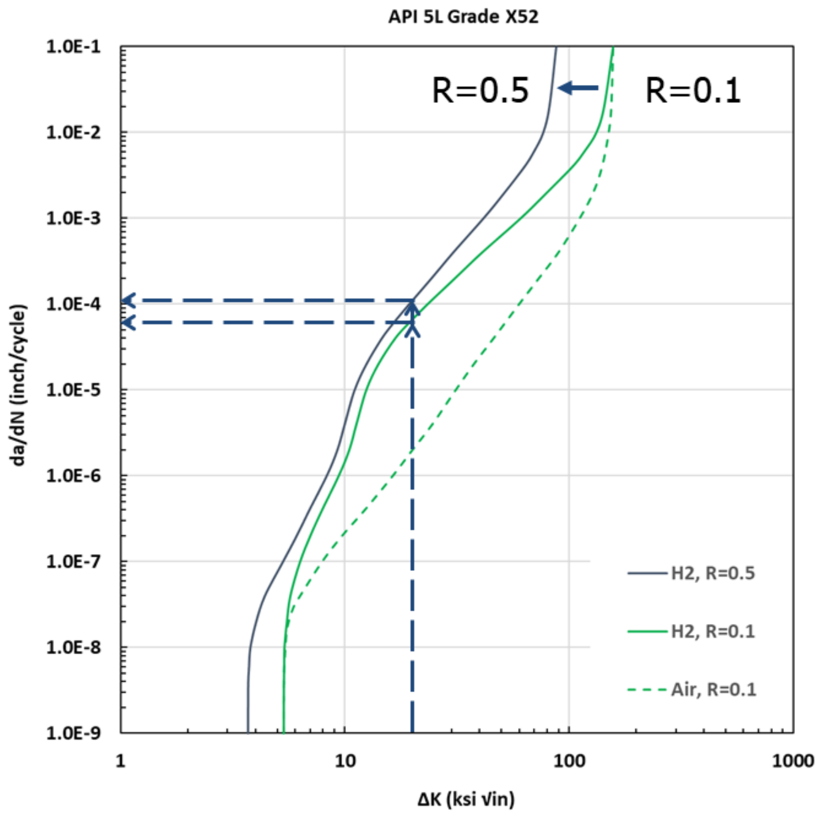

Figure 23. FCGR Affected by Residual Stress

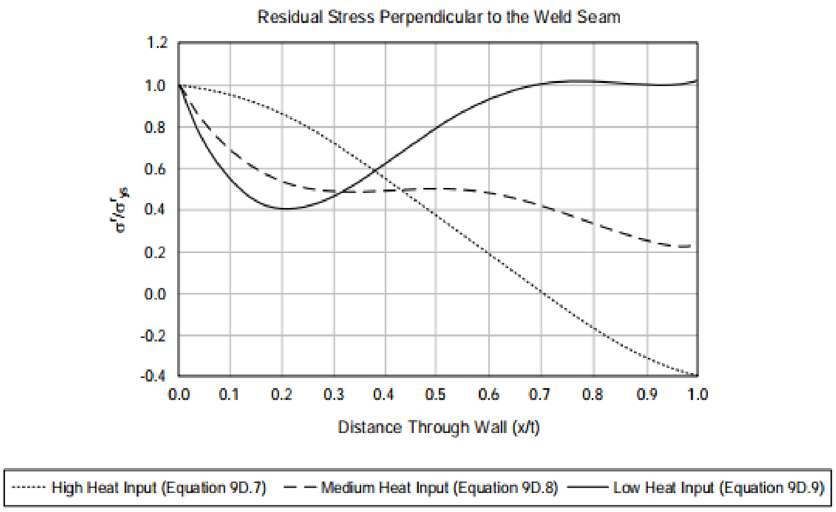

Figure 24. Residual Stress as a Function of Heat Input — Distribution Through WT (Reference API 579, Annex 9)

- Ronevich et al.[18,33] also showed that the distribution of weld residual stress through-thickness has periodicity with each weld pass.

- Residual stress is also position-dependent. As shown in Figure 25, the measured residual stress by Ronevich et al.[18,33] It is also a function of position along the fracture plane. For specimens taken from the BM, WFZ, and HAZ. Stress in the BM specimen (e.g., BM-9) was negligible throughout the entire width, whereas the WFZ specimens (e.g., W6 and W7) and HAZ specimens (e.g., H4 and H5) exhibited significant residual stresses.

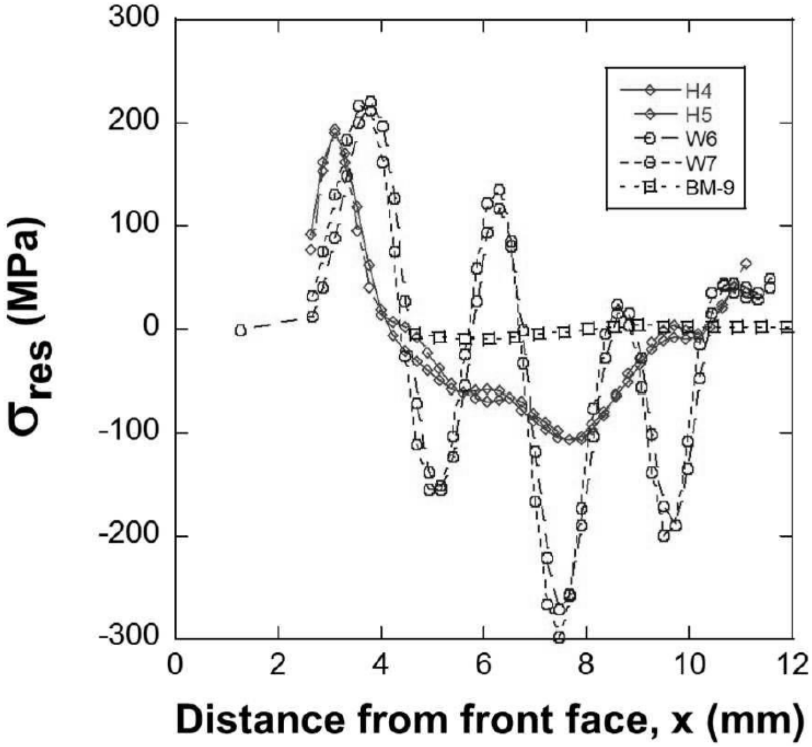

Figure 25. Measured Residual Stress as a Function of Distance from the Front Face

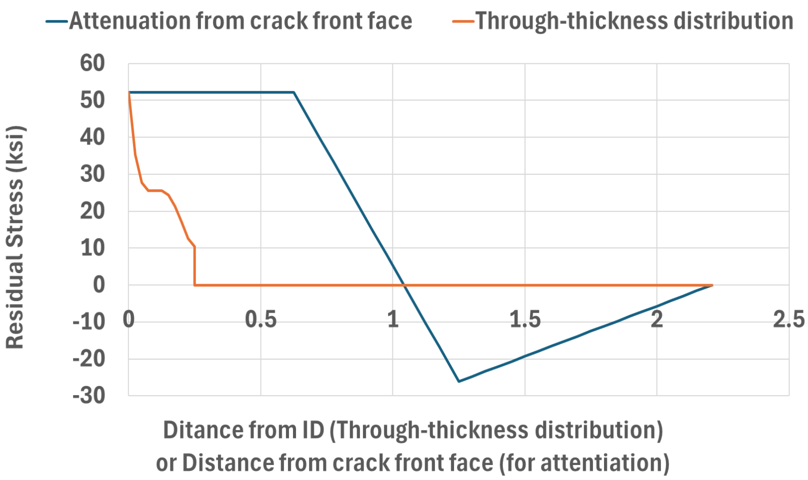

Figure 26. Example of Residual Stress Distribution Along Crack Depth and Front Face Used in the Parametric Studies for a 10-inch OD pipe of 0.25-inch WT, Grade X52, Medium Heat Input Assumption

A series of parametric studies was conducted to estimate the remaining fatigue life of girth welds while accounting for residual stresses and geometric stress concentrators, such as weld misalignment.

Laboratory and field data are limited for defining customized residual-stress inputs in hydrogen environments across the range of welding procedures and pipe grades considered in this study (X42, X52, and X60). Accordingly, the residual stress distribution was modeled in accordance with API 579 Annex 9D, which provides an upper-bound representation based on a literature survey of published results supplemented by numerical analysis. Fourth-order polynomial equations were used to represent progress through the depth, and piece-wise linear attenuation curves were used to represent progress in length (crack face front). A medium heat input was assumed for residual stress calculations, consistent with the applicable welding procedure specification (WPS) and the thickness ranges in our parametric studies. An example of residual stress distribution used in our studies is plotted in Figure 26.

Residual stresses were applied in each step of crack growth as a function of crack size. Residual stress intensity factors (residual K values) were obtained using the Gaussian integration technique. The results of the sensitivity studies for the girth weld RL with residual stress considerations are shown in Figure 27 for a 10-in OD, 0.25-in WT pipe using an aggressive pressure cycle (SSI = 147) regime.

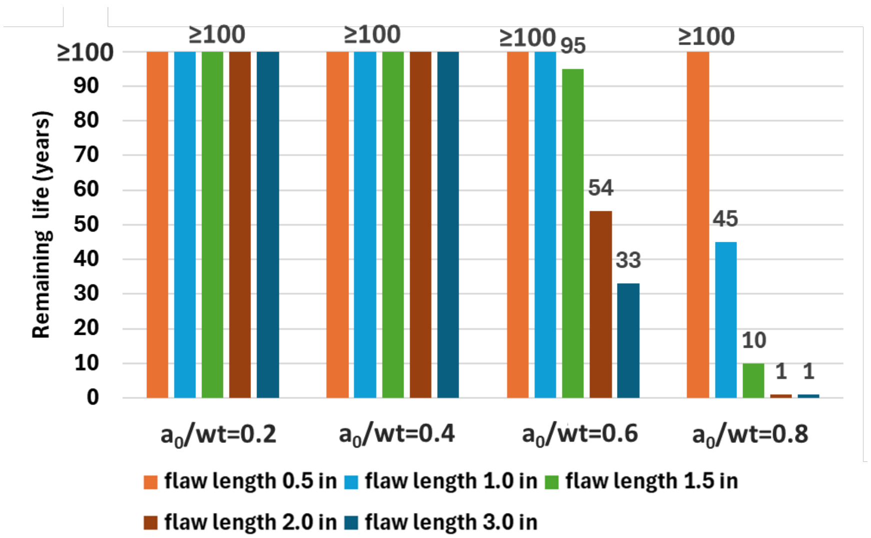

Figure 27. Remaining Fatigue Life of Girth Welds in a 10-in OD, 0.25-in WT, Grade X52 Pipe Under Aggressive Cycles

A comparison of Figure 20 (RL of circumferential crack-like features in the pipe body) with Figure 27 (girth weld) indicates that, under similar conditions, the presence of weld residual stress reduces RL, particularly for deeper, longer flaws. The results are highly sensitive to the assumed residual stress distribution. Specifically, the residual stress magnitude at the crack tip varies with its location relative to the weld centerline and the through-thickness weld pass profile. This, in turn, affects the effective R-ratio and consequently the FCGR.

As shown in Figures 28 and 29, under moderate and mild pressure cycling, girth welds subjected to residual stress exhibit longer fatigue lives. This indicates a less pronounced influence of residual stress compared to aggressive cycling conditions.

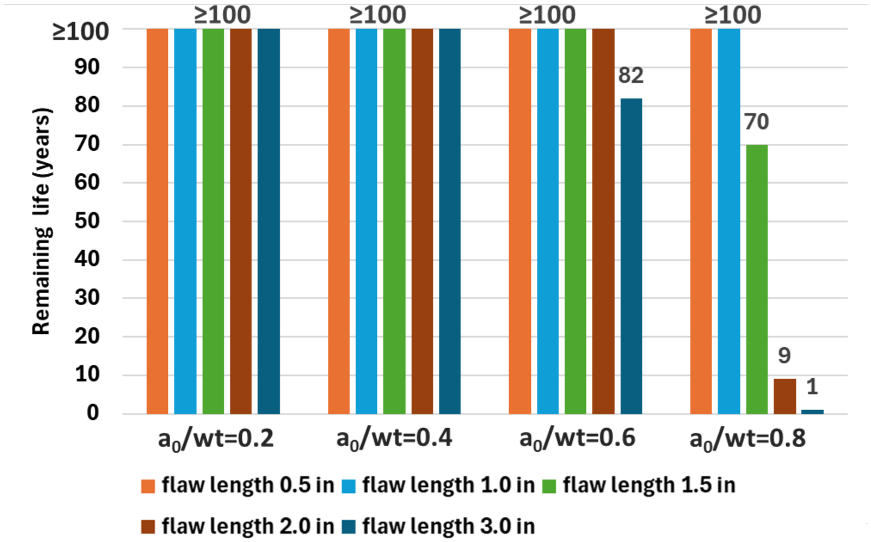

Figure 28. Remaining Fatigue Life of Girth Welds in a 10-in OD, 0.25-in WT, Grade X52 Pipe Under Moderate Cycles

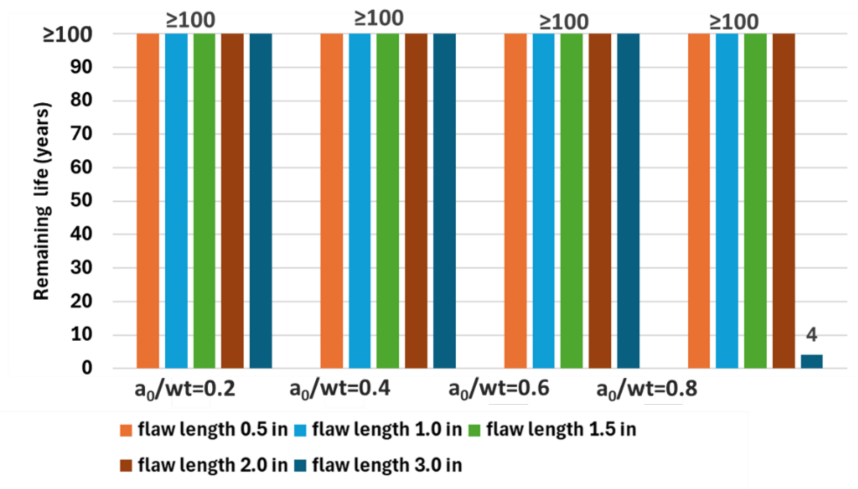

Figure 29. Remaining Fatigue Life of Girth Welds in a 10-in OD, 0.25-in WT, Grade X52 Pipe Under Mild Cycles

Residual stress increases with pipe yield strength (grade), resulting in higher weld residual stresses throughout the WT and along the crack front. An example is shown in Figure 30, based on the API 579 Annex 9D formulation (medium heat input) for a 10-in OD, 0.25-in WT pipe with grades X42, X52, and X60. Since WM is typically specified to overmatch the pipe grade (i.e., with higher yield and tensile strength), the resulting residual stress levels may exceed those estimated solely from the pipe grade.

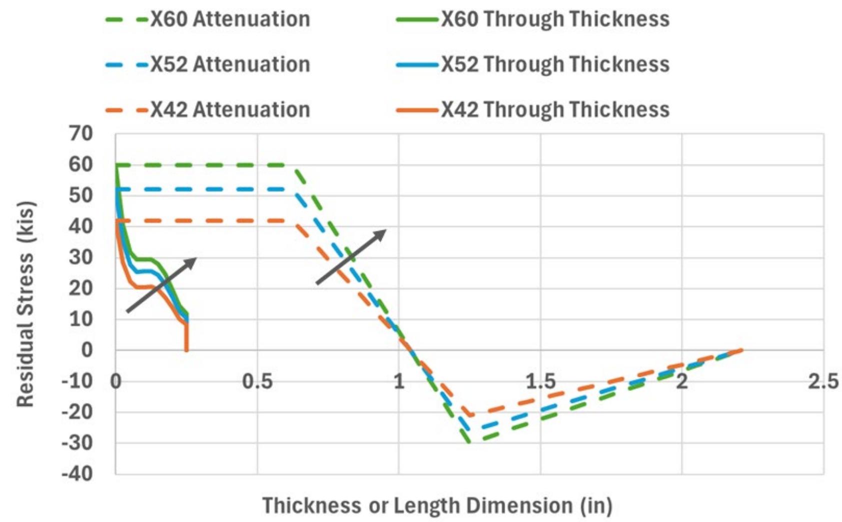

Figure 30. Residual Stress Distribution (Through Thickness and Along Crack Front Face) With Respect to Pipe Grade

The fatigue RL results for a 10-in OD, 0.25-in WT pipe under moderate pressure cycling with a 3-in flaw length showed a decreasing trend with increasing pipe grade, as illustrated in Figure 31. The same trend was observed in the sensitivity studies for Grade X42 (Figure 32) and Grade X60 (Figure 33). Comparison of these results with Figure 28 further confirms this consistent trend across different grades. This effect becomes more pronounced for deeper flaws, where higher pipe grades exhibit significantly reduced girth weld RL.

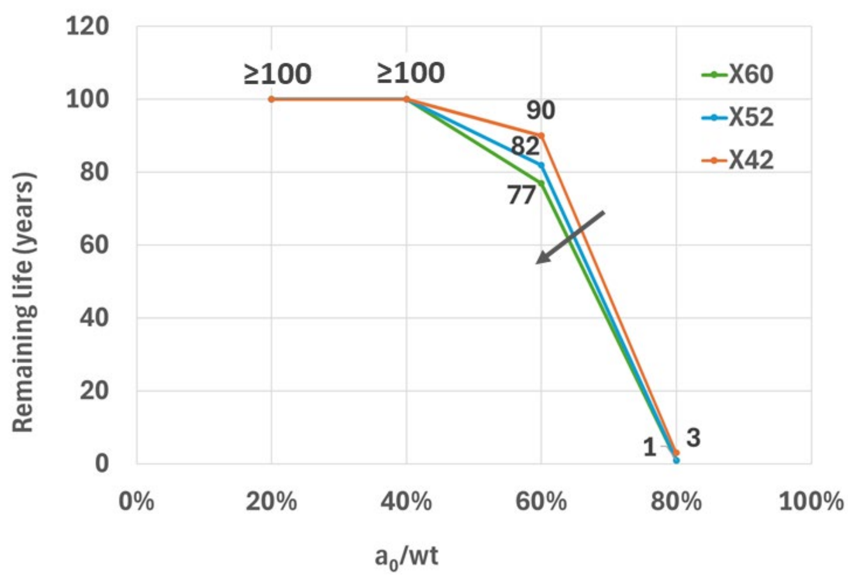

Figure 31. Remaining Fatigue Life of Girth Weld with Respect to Pipe Grade, in a 10-in OD, 0.25-in WT, Under Moderate Pressure Cycles with a 3-in Flaw Length

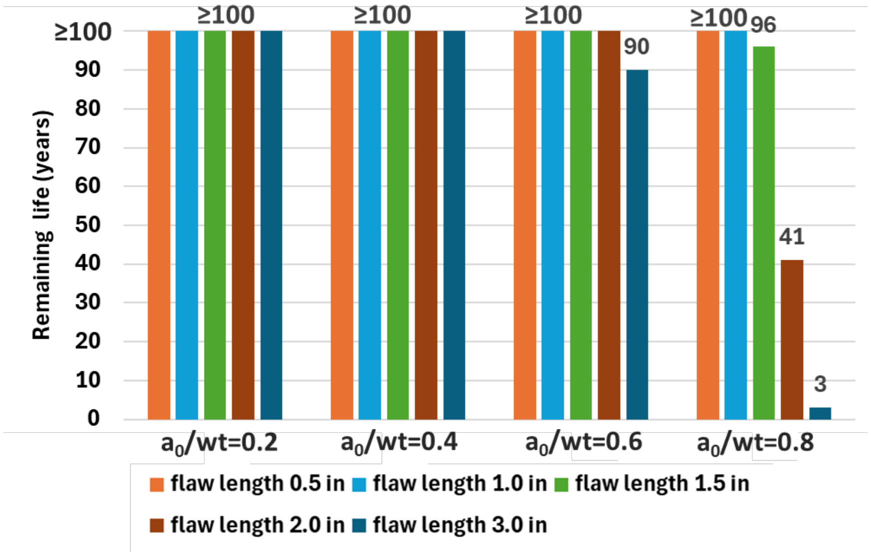

Figure 32. Remaining Fatigue Life of Girth Welds in a 10-in OD, 0.25-in WT, Grade X42 Pipe Under Moderate Cycles

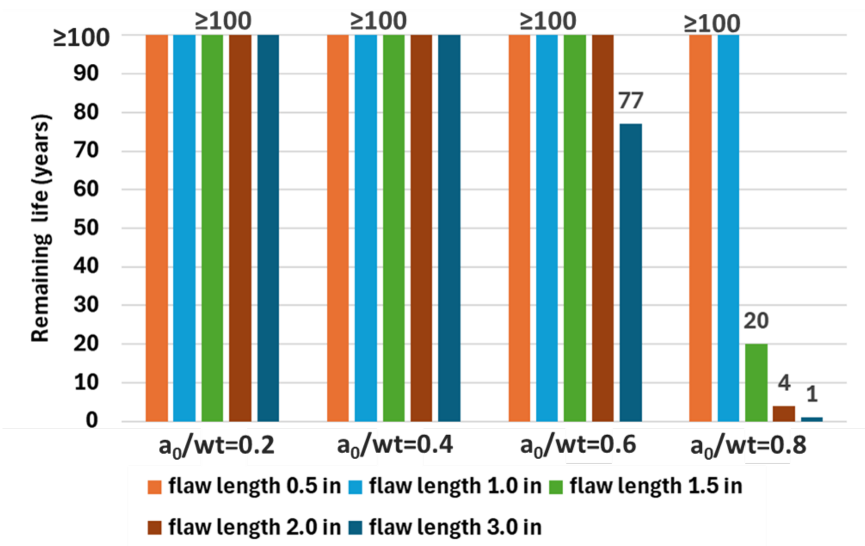

Figure 33. Remaining Fatigue Life of Girth Welds in a 10-in OD, 0.25-in WT, Grade X60 Pipe Under Moderate Cycles

5.3.2 Weld Misalignment

Weld misalignment (hi/lo) is a common feature in field/girth welds. Hi/lo conditions introduce localized stress concentrations. In this assessment, the effects of weld misalignment were evaluated in combination with weld residual stresses to capture their combined impact on crack driving force and fatigue crack growth behavior.

The influence of hi/lo was incorporated by using a stress concentration factor (SCF) to account for the geometric discontinuity at the weld. Depending on the formulation adopted (e.g., BS 7910[34]), representative SCF values for a 10-in OD, 0.25-in WT pipe range approximately from 1.3 to 2.7, based on API Specification 5L[10] dimensional tolerances. This is listed in Table 5.

Table 5. SCF Based on Weld HI-LO for a 10-in OD, 0.25-in WT Pipeline

HI-LO (inch)	HI-LO/WT	SCF based on BS 7910 formula
0.025	10%	1.3
0.063	25%	1.8
0.125	50%	2.7

The results in Figure 34 indicate that the inclusion of hi/lo increases the effective ΔK and, in the presence of tensile residual stresses, hi/lo conditions can further elevate the effective R-ratio. This combined effect accelerates fatigue crack growth and reduces the RL, with the impact becoming more pronounced for deeper flaws where stress concentration effects are more pronounced. Parametric evaluations confirm that this trend is consistent across a range of flaw sizes, pipe diameters, and pressure cycle severities, highlighting the importance of accounting for weld misalignment in fatigue and ECA assessments.

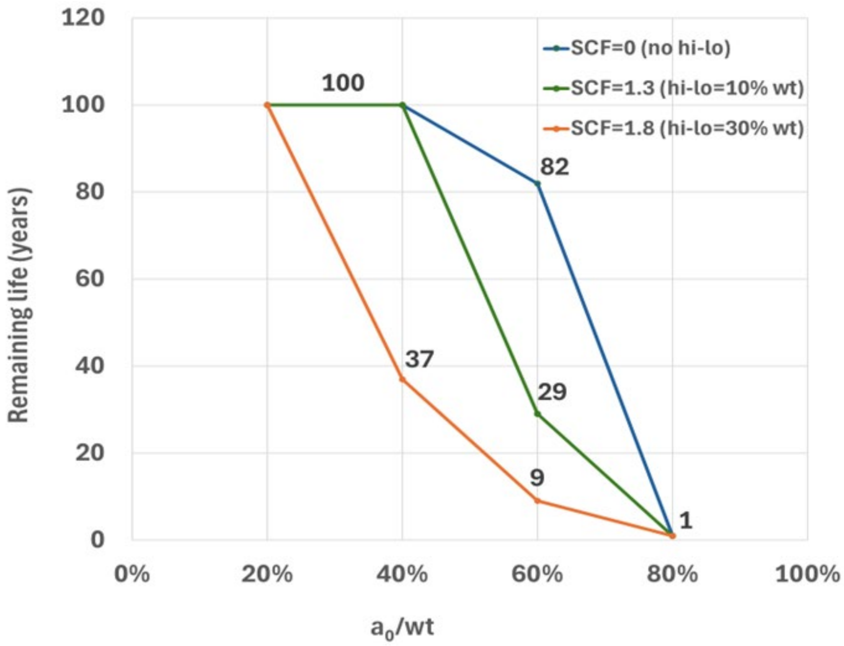

Figure 34. Remaining Fatigue Life of Girth Weld with HI-LO and Residual Stress Considerations in a 10-in OD, 0.25-in WT, with a 3-in Flaw Length Under Moderate Pressure Cycles

5.3.3 Low Fracture Toughness

So far, all case studies have been performed assuming a plane strain (K_{Ic}) fracture toughness of 90 ksi√in and a plane stress toughness (K_c) of 176 ksi√in. To account for cases of lower fracture toughness, particularly relevant for some vintage girth welds where Charpy V-notch (CVN) impact testing requirements were not consistently enforced, a broader range of lower fracture toughness values was considered.

Tables 6 and 7 presents the predicted fatigue RL of girth weld flaws as a function of fracture toughness for plane-strain/plane-stress conditions[vi] (expressed as K_{Ic} and K_c), comparing cases with and without weld residual stress.

The results effectively identify a threshold fracture toughness of approximately 30/45 ksi√in (plane-strain/plane-stress), below which brittle failure is likely. Above this fracture toughness threshold, the results are not very sensitive to toughness values, and predicted fatigue RL exceeds 100 years, even when weld residual stresses are included in the analysis.

For hydrogen-blend pipelines, these results are consistent with the requirements of ASME B31.12, which specify a minimum fracture toughness of ≥ 50 ksi√in (plane-strain).

Table 6. RL of Girth Welds with Varying Fracture Toughness under Mild Pressure Cycles, in a 10-in OD, 0.25-in WT Pipeline, with a 3-in Flaw Length

K_{Ic}/K_c (ksi√in)	Remaining life with residual stress	Remaining life No residual stress
20/30	<1	>100
25/38	<1	>100
30/45	>100	>100
40/60	>100	>100
50/75	>100	>100
90/135	>100	>100

Table 7. RL of Girth Welds with Varying Fracture Toughness under Moderate Pressure Cycles, in a 10-in OD, 0.25-in WT Pipeline, with a 3-in Flaw Length

K_{Ic}/K_c (ksi√in)	Remaining life with residual stress	Remaining life No residual stress
20/30	<1	<1
25/38	<1	>100
30/45	>100	>100
40/60	>100	>100
50/75	>100	>100
90/135	>100	>100

5.3.4 Summary

Considerations for the RL of girth welds in hydrogen service:

- Hydrogen blending increases sensitivity to:
  - Residual tensile stress;
  - Geometric stress concentrations (e.g., weld misalignment);

[vi] See Section 3.4 for the definition of apparent fracture toughness as a combination of plane-strain and plane-stress toughness.

    - Flaw size; and
    - The combined effect of pipe grade, residual stress, and weld misalignment can reduce RL if not controlled.
- Enhanced inspection of girth welds should be prioritized in:
    - Non-PWHT welds and high-grade pipe segments;
    - Locations with known fit-up challenges; and
    - Areas subject to higher cyclic pressure fluctuations.
- Consideration should be given to improved welding procedures and tighter construction quality assurance/quality control (QA/QC) requirements for hydrogen systems.

6 FATIGUE REMAINING LIFE OF DENTS

6.1 Integrity Assessment of Dents in Hydrogen and Blend Pipelines

Dents, gouges, and wrinkles all significantly increase the risk of crack initiation in hydrogen environments. Mechanical dents introduce stress concentration zones, and when combined with hydrogen embrittlement, these areas become critical failure points.

Dents in pipelines can lead to several primary failure mechanisms, depending on the severity of deformation, material properties, and operating conditions. As shown in Figure 35, the main failure modes in dents include:

- Crack initiation during dent formation;

  Significant plastic deformation associated with dent formation can generate sufficient strain to initiate cracks, particularly at locations of high local strain concentration.

  The presence of hydrogen exacerbates this failure mechanism. Zhao and Cheng[35] showed that increased hydrogen atom concentration reduces the resistance to crack initiation, allowing cracks in hydrogen pipelines to form at smaller indentation levels than in natural gas pipelines.
- Fatigue under cyclic loading; and

  Repeated pressure cycling can lead to fatigue crack initiation and propagation within the dented region. This is typically the dominant failure mechanism for in-service dents and is the primary focus of most integrity assessments in natural gas pipelines.

  The presence of hydrogen further intensifies this failure mechanism by increasing the FCGR and reducing the critical crack size through a decrease in fracture toughness.
- Reduction in failure pressure.

  The presence of a dent can reduce a pipeline's burst capacity, especially when combined with other features such as cracks or material degradation. The presence of hydrogen can further reduce the failure pressure by lowering fracture toughness.

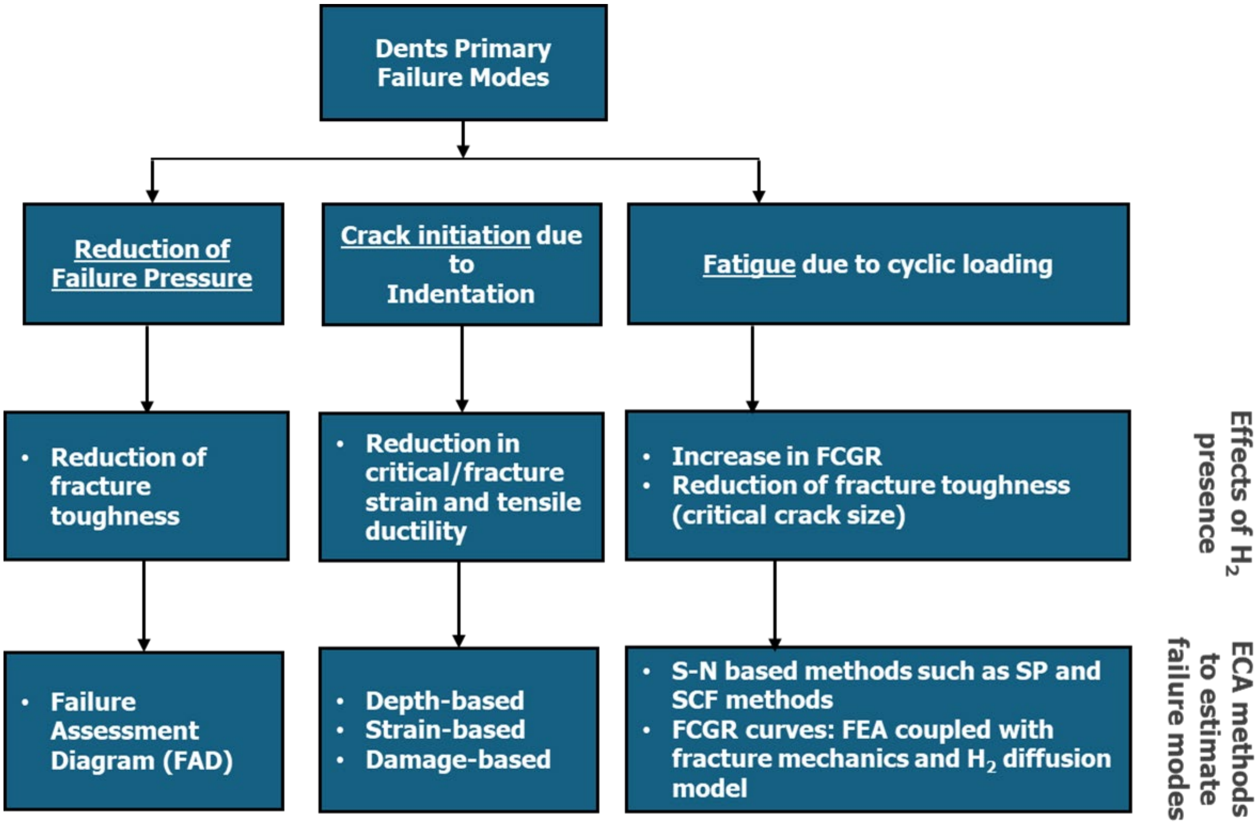

Figure 35. Dent Primary Modes of Failure and How Hydrogen Affects It

Due to the increased severity of dent behavior in hydrogen environments, more restrictive acceptance criteria are required. Dents that may have previously been considered non-injurious in natural gas service may become critical when exposed to hydrogen.

This shift increases the reliance on detailed ECAs, which require high-quality input data, including:

- High-resolution three-dimensional dent profiles;
- Pressure cycle histories with sufficient resolution; and
- Material testing (Level 3 ECA is expected to be required more often in hydrogen service than in natural gas service).

Several additional factors must be considered when evaluating dents in hydrogen service:

- Reduced allowable dent depth: Traditional acceptance limits (e.g., 6% dent depth) may no longer be applicable, as crack initiation can occur at smaller deformation levels as reported by Zhao and Cheng.[35,36]
- Reduced ductility and strain capacity: Hydrogen exposure lowers tensile ductility and critical strain, requiring more restrictive strain-based criteria. This is plotted in Figure 36 from studies performed by Zhao and Cheng.[35,36]
- Earlier crack initiation: It is shown that increased hydrogen concentration reduces the indentation displacement required for crack initiation.
- Hydrogen distribution effects: Hydrogen accumulation is influenced by local plastic strain and hydrostatic stress, both of which are elevated in dented regions.

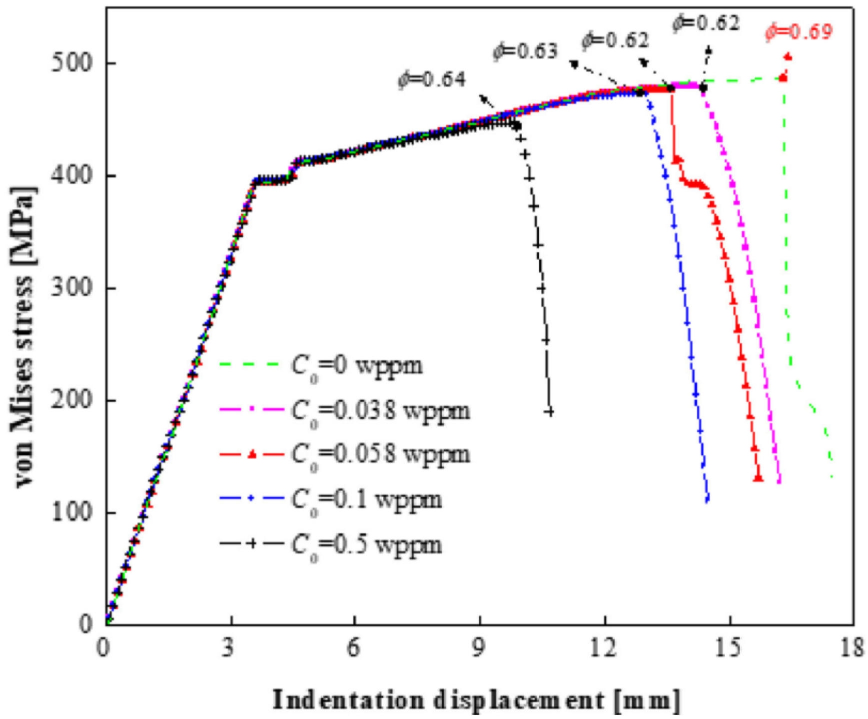

Figure 36. Effect of Hydrogen Concentration on Ductility and Strain Capacity of Dented Pipes[35]

- The interaction between dents and crack-like features significantly reduces local burst capacity. This effect is more pronounced in hydrogen service due to the combined effects of reduced ductility, increased crack-growth susceptibility, and elevated crack-driving forces.

Accordingly, dent assessment in hydrogen pipelines requires more restrictive criteria and a more detailed analytical approach to ensure safe and reliable operation.

6.2 Fatigue Assessment of Dents in Hydrogen and Blend Pipelines

Fatigue analysis of dents in hydrogen pipelines differs from that in natural gas systems due to the increased susceptibility to crack initiation and growth under hydrogen exposure.

In the S–N approach, discussed in Section 2.3.1, fatigue behavior is characterized by the relationship between stress range and the number of cycles to failure. As expected, the data indicated that fatigue life in hydrogen environments is reduced compared to air, with the hydrogen curve lying below the air curve. The corresponding S–N parameters (slope m and intercept C) can be obtained through regression, reflecting a steeper fatigue response in hydrogen.

From a practical standpoint, S–N methods are often preferred for plain dent assessments because a significant portion of fatigue life is typically consumed during the crack initiation phase. This is consistent with the observed data, which show that, in hydrogen environments, most of the fatigue life occurs during crack initiation (Figure 37). However, the applicability of S-N methods in hydrogen service is subject to greater uncertainty, as hydrogen can alter endurance behavior through mechanisms such as embrittlement and accelerated crack initiation.

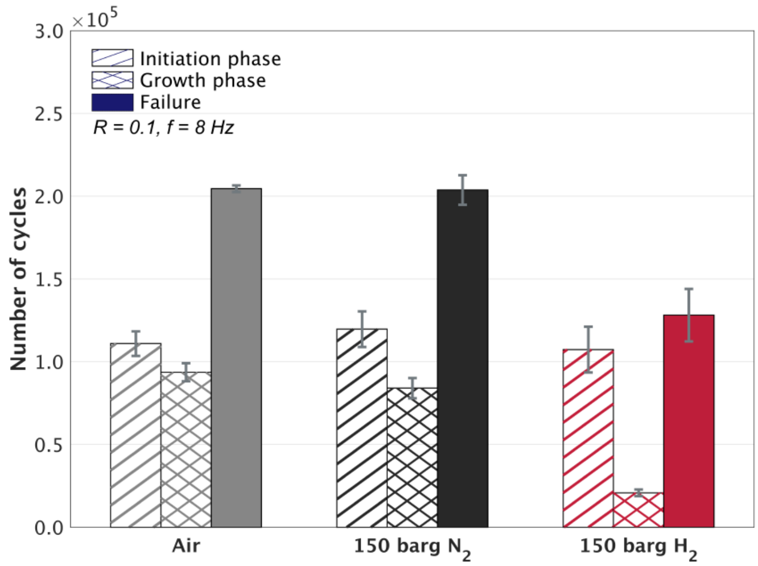

Figure 37. Number of Cycles in the Crack Initiation Phase and Growth Phase in Air and Hydrogen[37]

Fracture mechanics-based fatigue approaches provide a more rigorous and physically representative framework, particularly for cases involving pre-existing crack-like features such as a dent with a gouge. In dented regions, the stress field is highly non-uniform, and in hydrogen service, this is further complicated by the interaction between stress/strain fields and hydrogen concentration and diffusion, necessitating coupled multi-physics considerations. As a result, more advanced (e.g., Level 3) ECA approaches are often required for hydrogen applications compared to conventional natural gas systems. A summary of these considerations is listed in Table 8.

The application of SFs is critical in both approaches. Depending on the level of assessment and the availability of material data, SFs ranging from 2 to 5 [49 CFR 192.712(c)] are commonly applied to predicted RL to define reassessment intervals. For dents in hydrogen service, higher SFs are generally warranted due to increased susceptibility to crack initiation and growth, as well as greater uncertainty in material behavior.

Table 8. Methods for Fatigue Assessment of Dents

Aspect	S–N Methods	Fracture Mechanics Methods for FCGR
Basis	Empirical S–N curves (stress range → cycles to failure) Shape Parameter (SP) methods[38] Stress Concentration Factor (SCF) methods[38]	Fatigue crack growth rate (da/dN) vs stress intensity ΔK
Defects Covered	Implicitly accounts for initiation + growth	Explicitly models crack initiation & growth
Inputs Required	Stress range, SCF/shape factor, material S-N curve in H_2	ΔK calculation, FCGR curve in H_2
Complexity	Simpler, more practical, but more conservative (+2 STD) (H_2 environment alters endurance curves due to embrittlement and faster initiation)	More complex, requires FEA & fracture mechanics. More reliable but challenging: H_2 concentration varies with stress field in dent → multi-physics coupling needed

7 RECOMMENDED FUTURE STUDIES

The present study provides a practical basis for developing reassessment intervals in hydrogen service. Additional research is recommended in several areas to improve technical confidence, reduce uncertainty, and better support the implementation of hydrogen services within IMPs.

Probabilistic fatigue assessment:

- RIs in hydrogen service would benefit from a probabilistic framework that explicitly accounts for uncertainty in flaw size, POD, probability of identification (POI), ILI/NDE sizing error, fracture toughness, FCGR scatter, residual stress, and pressure history. Tools like the publicly available HELPR software[39], developed as part of the SNL HyBlend Project, can facilitate such analyses using ASME B31.12 hydrogen FCGR design curves, as described by Schroeder et al.[40] Expanding these platforms to support actual FCGR test data would provide a significant advantage.

  A practical next step would be to extend tools like this to allow the use of measured hydrogen FCGR datasets in addition to ASME B31.12 design curves and then link the output directly to reassessment interval selection and risk ranking. This would be especially valuable for features near action thresholds, where uncertainty often drives conservative decisions more than the mean prediction itself.

Hard spots in hydrogen and hydrogen-blended service:

- Recent studies show that hard spots remain a credible integrity threat, especially in vintage pipes, and that the susceptibility envelope is broader than previously assumed. Current operator experience and the 2024 PHMSA advisory bulletin[41] on the assessment of hard spots both indicate that hard spots can interact with coating degradation, soil chemistry, stress, and increased hydrogen exposure to promote HIC.

  A focused program should therefore be undertaken for hard spots in hydrogen and hydrogen-blended service. The work should quantify the relationship among local hardness, microstructure, through-wall extent, fracture resistance, and hydrogen-assisted crack initiation/growth. This is especially important for vintage assets, where hard spots may remain stable for long periods unless acted upon by coincident factors such as coating degradation, local stress, and atomic hydrogen. Recent pipeline conference literature shows that hard spots with sufficiently high hardness may be susceptible to hydrogen embrittlement and hydrogen stress cracking, and that operators are actively pursuing hard spot identification, validation, and mitigation programs.[42,43]

Hydrogen concentration:

- At high driving force (i.e., high ΔK), the fatigue crack growth is independent of pressure and an order of magnitude greater than in air, even for hydrogen partial pressure as low as 0.1 MPa. Indeed, hydrogen embrittlement occurs even at low blend concentrations. The current effort in Code Development for B31.8 and B31.12 considers any concentration of intentionally added hydrogen gas to be potentially detrimental and conservatively prescribes design as if the pipeline were exposed to 100% hydrogen partial pressure. Similarly, this study also focused on 100% hydrogen gas conditions. However, lower hydrogen concentrations (e.g., 1% or 10%) have also been shown to moderately reduce FCGR and fracture toughness in the intermediate ΔK range.[44]

Therefore, a useful next phase would be to generate engineering crack-growth models for hydrogen blends and mixed-gas conditions, including low and intermediate hydrogen concentrations, pressure dependence, and the possible role of impurities. That work should aim to establish when 100% hydrogen remains an acceptable conservative surrogate and when it becomes overly conservative for reinspection planning. Recent work published at industry workshops and conferences such as the ASME Pressure Vessel and Piping (PVP) conference, the Association For Materials Protection And Prevention (AMPP) conference, and the International Pipeline Conference (IPC) indicates that methane-hydrogen mixtures and gas pressure measurably affect FCGR behavior, which makes this a high-value area for follow-on testing and model calibration.[45,46,47]

Low-cycle fatigue:

- Future work should expand the current pressure-cycling treatment to include low-cycle fatigue associated with relatively infrequent but high-severity transient events, including start-ups, shutdowns, station recycling, blowdowns, and other non-steady operating events. These events can impose large pressure fluctuations compared with routine steady-state cycling and may therefore contribute disproportionately to crack initiation and early crack extension, particularly in hydrogen service, where fatigue crack growth is accelerated.

  A useful next step would be to build event-based pressure-history libraries and evaluate their effect on RL separately from routine cyclic operation, rather than treating all pressure fluctuations through a single annual severity metric. Future studies should therefore determine when transient-event loading governs reassessment intervals, how such events should be counted or modeled, and whether hydrogen-service IM requires separate criteria for routine cycling versus transient low-cycle fatigue demand.

8 CONCLUSION AND SUMMARY

The transition from natural gas service to hydrogen or blended hydrogen/natural gas service requires a reassessment of how IM RIs are established. Hydrogen affects pipeline integrity in ways that are not adequately captured by conventional natural gas assumptions, primarily through accelerated fatigue crack growth, reduced fracture resistance, and increased sensitivity of existing flaws to cyclic loading. As a result, crack-like features that may remain stable or slow-growing in natural gas service can exhibit shorter RL in hydrogen environments.

From an IM perspective, the objective remains unchanged: detected features must be managed such that reinspection or mitigation occurs before they reach critical size. RL is therefore the controlling parameter, and the RI must be set shorter than the estimated RL by applying an appropriate SF. The choice of SF depends on several considerations, including confidence in the material inputs, the assessment methodology, and the consequences of failure. For example, when average or typical industry material properties are used without laboratory verification, a larger SF may be warranted than when minimum material properties and upper-bound FCGR data are applied. As a result, all else being equal, the RI would be shorter in the former case than in the latter.

This study was undertaken to provide a more technically defensible basis for reassessment in hydrogen service through a combination of fracture mechanics-based fatigue analysis and targeted sensitivity studies as described below:

- The analysis used advanced crack growth models capable of representing behavior across the full fatigue spectrum, Regions I, II, and III. The analysis used the Harter T-method (an extension of the Walker method), used mainly in the aerospace industry, and implemented in AFGROW software, incorporated Sandia National Laboratories' hydrogen FCGR and fracture toughness data to improve realism, and reduced conservatism relative to sole reliance on upper-bound design curves such as ASME B31.12, Code Case 220.
- Sensitivity analyses were performed over a practical range of parameters, including flaw depth (5% to 80% of WT) and length (0.5 to 3.0 in.), fracture toughness (20 to 90 ksi√in), pipe geometry (10-in. OD × 0.25-in. WT and 20-in. OD × 0.50-in. WT), and pressure cycle severity (mild, moderate, and severe cycles). The work also considered flaw sizes near and below practical ILI/NDE detection thresholds, recognizing that undetected subcritical flaws are also important for RI determination.
- The sensitivity studies were conducted assuming 100% hydrogen, since experimental results[21,22] show that even small amounts of hydrogen (1% to 5%) can adversely affect material properties, including fracture toughness and FCGR.

The results showed that:

- Fatigue life in hydrogen gas is approximately one order of magnitude less than in air across the pipe geometries and pressure spectra considered.
- For longitudinal crack-like flaws, long fatigue lives were predicted for relatively small flaws under mild pressure cycling, indicating that not all features become immediately limiting in hydrogen service. In these mild-cycling cases, conservative upper-bound methods remain appropriate for populations of smaller flaws.
- However, under aggressive pressure cycling, for deeper flaws, and for lower-toughness materials, RL in hydrogen service decreases substantially, supporting shorter RIs, and, for such cases, a more detailed analysis using actual hydrogen FCGR data would be beneficial.
- Pipe geometry and material condition were shown to remain important controlling variables in hydrogen service. Thinner-wall pipes exhibited shorter fatigue life because of the smaller remaining ligament at a given normalized flaw depth, whereas larger-diameter, thicker-wall pipes with the same OD/WT ratio generally showed longer life for larger flaws.
- Reducing fracture toughness in hydrogen service from the base-case average level (90 ksi√in) to the ASME B31.12 specified minimum (50 ksi√in) had only a modest effect in many of the longitudinal flaws, but further reductions in toughness below the minimum limit (<50 ksi√in) led to much shorter RL.
- Most longitudinal flaw failures in hydrogen service occurred after the crack depth became effectively through-wall, indicating a generally favorable leak-before-break response, but one that still depends on timely detection and reassessment.
- Girth welds and other field welds require special attention in hydrogen service. Relative to comparable pipe-body flaws, weld flaws are more sensitive to hydrogen because of the combined influence of flaw size, residual tensile stress, weld misalignment, and, in some cases, lower or more variable fracture toughness associated with vintage welds.
- The combined effect of pipe grade, residual stress, and geometric stress concentration can substantially reduce the RL of girth welds in hydrogen service. Accordingly, enhanced inspection and reassessment of girth welds should be prioritized in non-PWHT welds, high-grade pipe segments, locations with known fit-up challenges, and areas subject to higher

cyclic pressure fluctuations. These findings also support improved welding procedures and tighter construction QA/QC requirements for hydrogen systems.

- In addition to crack-like flaws in the pipe body and welds, this study indicated that dents and related mechanical damage features should be assessed more conservatively for pipelines in hydrogen service. Hydrogen increases susceptibility to crack initiation and can reduce the deformation threshold at which dents become injurious. As a result, damage features that may have been acceptable in natural gas service may require re-evaluation, shorter reassessment intervals, or more advanced ECA methods when hydrogen is present.
- Overall, simplified conservative methods and inputs such as ASME B31.12 Code Case 220 remain useful for screening smaller flaws under mild to moderate pressure cycle conditions. However, larger flaws, aggressive pressure cycling, low-toughness materials, and weld-related imperfections often justify more refined fracture mechanics-based analysis using realistic hydrogen FCGR data.

The practical implication is that hydrogen service does not require a uniform reduction in RIs for all mechanical integrity threats and may not require the use of advanced fatigue assessment methods. However, it does require a more targeted, technically rigorous approach to identify which inputs, features, and operating conditions will govern reassessment timing.

Additional future work is recommended to further strengthen the technical basis for reassessment interval development in hydrogen service:

- Priority areas include probabilistic methods for RI determination; hydrogen-specific evaluation of hard spots; the effects of hydrogen concentration and blended-gas composition on crack growth; and treatment of low-cycle fatigue associated with transient operating events such as start-ups, shutdowns, station recycling, blowdowns, and other non-steady conditions.

9 REFERENCES

[1] Brongers, M. (2024, July 26). *Literature review on reinspection intervals for pipelines carrying hydrogen or hydrogen/natural gas blends* (Task 1 Final Report No. 24-30994-5000932R). Kiefner and Associates, Inc.; U.S. Department of Transportation Pipeline and Hazardous Materials Safety Administration.

[2] Brongers, M. P. (2025, June 23). *Evaluation of analyses for different hydrogen/natural gas blends* (Task 5 Final Report No. 25-30994-6000754R). Kiefner and Associates, Inc.; U.S. Department of Transportation Pipeline and Hazardous Materials Safety Administration.

[3] American Society of Mechanical Engineers. (2025). *Managing system integrity of gas pipelines* (ASME B31.8S-2025).

[4] Rana, A., Tiku, S., Dinovitzer, A., Piazza, M., & Burns, T. (2022, June 6–10). *Mechanical damage fatigue and formation cracking assessment techniques* [Paper presentation]. EPRG-PRCI-APGA 23rd Joint Technical Meeting, Edinburgh, Scotland.

[5] Hill, L., Bagnoli, K., Twombly, E., Punch, E., Gao, X., & Wilkowski, G. (2024, September 23–27). *Sensitivity studies on the evaluations of hydrogen effects on linepipe integrity challenges* [Paper presentation]. ASME 2024 International Pipeline Conference (IPC), Calgary, AB, Canada. https://doi.org/10.1115/IPC2024-134020

[6] San Marchi, C., Ronevich, J., Schroeder, B., Devin, M., Davis, B., & Agnani, M. (2023, December 6). *HyBlend - Overview: Hydrogen-assisted fatigue and fracture of line pipe steels* [Presentation]. Sandia National Laboratories.

[7] American Society of Mechanical Engineers. (2023). *Code for hydrogen piping and pipelines* (ASME B31.12-2023).

[8] Smart, L., & Brongers, M. P. (2025, December 11). *Evaluation of analyses for hydrogen relevant threats* (Task 6 Draft Report No. 24-30994-6000754R-Rev1). Kiefner and Associates, Inc. for U.S. DOT PHMSA.

[9] Novitech, Inc. (2024, October). *Data on flaws detected by different ILI techniques: Micron MFL and deformation ILI tools*.

[10] American Petroleum Institute. (n.d.). *Specification for line pipe* (API SPEC 5L).

[11] American Petroleum Institute & American Society of Mechanical Engineers. (2021, December). *Fitness-for-service* (API 579-1/ASME FFS-1-2021).

[12] DNV. (n.d.). *CorLAS™: Crack failure pressure calculator* [Software]. https://www.dnv.com/oilgas/pipelines/digital-pipeline-tools/

[13] American Society of Mechanical Engineers. (2023, July 10). *Code Case 220 for ASME B31.12 hydrogen piping and pipelines - Fatigue crack growth rate properties in hydrogen for B31.12 pipeline materials* (CC-220).

[14] Lextech, Inc. (n.d.). *AFMAT fracture mechanics database* [Database].

[15] Lextech, Inc. (n.d.). *AFGROW software tool for fatigue crack growth analysis* [Software].

[16] Harter, J., & Lamborn, L. (2023, March 7). *Pipeline steel tubular da/dN curves with validations, hydrogen application* [Paper presentation]. PRCI 2023 Research Exchange, Houston, TX.

[17] Harter, J., & Lamborn, L. (2023, March 7). *Pipeline steel tubular da/dN curves with validations, hydrogen application* [Presentation]. PRCI 2023 Research Exchange, Houston, TX.

[18] Ronevich, J. A., & Somerday, B. P. (2016, September 6). Assessing gaseous hydrogen assisted fatigue crack growth susceptibility of pipeline steel weld fusion zones and heat affected zones. *Materials Performance and Characterization, 5*(3), 290–304. http://dx.doi.org/10/1520/MPC20150057

[19] Stalheim, D., Boggess, T., Bromley, D., Jansto, S., & Ningileri, S. (2012, September 24–28). *Continued microstructure and mechanical property performance evaluation of commercial grade API pipeline steels in high pressure gaseous hydrogen* [Paper presentation]. ASME 2012 International Pipeline Conference (IPC), Calgary, AB, Canada. https://doi.org/10.1115/IPC2012-90313

[20] Ronevich, J. A., Song, E. J., Somerday, B. P., & San Marchi, C. W. (2020). *Hydrogen-assisted fracture resistance of pipeline welds in gaseous hydrogen* (SAND2020-14066J). Sandia National Laboratories.

[21] PVP2021-62045, Materials Compatibility Concerns for Hydrogen Blended into Natural Gas, J.A. Ronevich, C. San Marchi, American Society of Mechanical Engineers (ASME), Virtual, Online, ASME 2021 Pressure Vessels and Piping Conference, 13-15 July, 2021.

[22] PVP2018-84658, Influence of Hydrogen and Oxygen Impurity Content in a Natural Gas/Hydrogen Blend on the Toughness of an API X70 Steel, L. Briottet, H. Ez-Zaki, American Society of Mechanical Engineers (ASME), Prague, Czech Republic, ASME 2018 Pressure Vessels and Piping Conference, 15-20 July, 2018.

[23] Ronevich, J. A., Somerday, B. P., & Feng, Z. (2017, February 16). Hydrogen accelerated fatigue crack growth of friction stir welded X52 steel pipe. *International Journal of Hydrogen Energy, 42*(7), 4259–4268. https://doi.org/10.1016/j.ijhydene.2016.10.153

[24] IPC2018-78717. Semiga, V., Dinovitzer, A., Tiku, S., & Gignal, G. (2018, September 24–28). *Liquid pipeline location specific cyclic pressure determination* [Paper presentation]. ASME 2018 International Pipeline Conference (IPC), Calgary, AB, Canada.

[25] Holbrook, J., & Cialone, H. (1985, February 15). *Effects of SNG/hydrogen gas mixtures on high pressure pipelines* (NG-18 Report No. 151). Battelle Columbus Laboratory for American Gas Association.

[26] Ward, L., Sugden, R., & Brongers, M. P. (2025, September 9). *Recommended revisions in 49 CFR 192, ASME B31.8, and ASME B31.8S* (Task 3 Final Report No. 25-30994-6000754R). Kiefner and Associates, Inc. for U.S. DOT PHMSA.

[27] Canadian Energy Pipeline Association. (2007, December). *Stress corrosion cracking - Recommended practices* (2nd ed.).

[28] Lamborn, L. (2025, April 28). *Unification of NNPH stress corrosion cracking, corrosion fatigue, and free hydrogen environment growth models* [Presentation]. API Pipeline Conference and Expo, Austin, TX.

[29] Lamborn, L., Krug, B., Nagra, G., Wong, D., & Vorontsov, V. (2025, July 20–25). *Crack threat management transition from hydrostatic test to in-line inspection for an aging pipeline* [Paper presentation]. ASME 2025 Pressure Vessels and Piping Conference, Montreal, QC, Canada. https://doi.org/10.1115/PVP2025-154677

[30] Fessler, R., & Batte, A. D. (2013). *Criteria for susceptibility to circumferential SCC* (Final Report 113603-R01). Pipeline Research Council International.

[31] Lamborn, L., Hogan, J., Ferguson, J., & Skow, J. (2024, July 28–August 2). *Circumferential and off-axis crack fatigue growth susceptibility in buried steel pipelines* [Paper presentation]. ASME 2024 Pressure Vessels and Piping Conference, Bellevue, WA. https://doi.org/10.1115/PVP2024-122643

[32] Thompson, R., Corbett, A., Solano, G., & Kania, R. (2024, February 12–16). *Integrity management of off-axis SCC through an ILI system and engineering assessment* [Paper presentation]. Pipeline Pigging and Integrity Management Conference (PPIM) 2024, Houston, TX.

[33] Ronevich, J. A., D'Elia, C. R., & Hill, M. R. (2018, May 1). Fatigue crack growth rates of X100 steel welds in high pressure hydrogen gas considering residual stress effects. *Engineering Fracture Mechanics, 194*, 42–51. https://doi.org/10.1016/j.engfracmech.2018.02.030

[34] British Standards Institution. (2019, December 31). *Guide to methods for assessing the acceptability of flaws in metallic structures* (BS 7910:2019).

[35] Zhao, J., & Cheng, Y. F. (2024). A phase field method for predicting hydrogen-induced cracking on pipelines. *International Journal of Mechanical Sciences, 283*, 109651. https://doi.org/10.1016/j.ijmecsci.2024.109651

[36] Zhao, J., & Cheng, Y. F. (2023, September 7). Finite element modeling of the distribution of hydrogen atoms at a dent on pipelines for hydrogen transport under cyclic loading. *International Journal of Fracture, 246*, 181–201.

[37] Faucon, L. E., Boot, T., Riemslag, T., Scott, S. P., Liu, P., & Popovich, V. (2023, March 10). Hydrogen-accelerated fatigue of API X60 pipeline steel and its weld. *Metals, 13*(563). https://doi.org/10.3390/met13030563

[38] Tiku, S., Ashraghi, A., Dinovitzer, A., & Rana, A. (2018, December 20). *Fatigue life assessment of dents with and without interacting features* (Final Report PR 214-114500-R01). BMT Canada Ltd. for PRCI. https://doi.org/10.55274/R0011540

[39] Schroeder, B. (2024, July 31–August 1). *An overview of the hydrogen extremely low probability of rupture (HELPR) toolkit for probabilistic structural integrity assessments when transporting hydrogen in natural gas infrastructure* [Presentation]. ASME 2024 Pressure Vessels and Piping Conference, Bellevue, WA.

[40] Schroeder, B., San Marchi, C., Ronevich, J., Devin, M., Duell, J., & Potts, S. (2024, July 28–August 2). *Utilizing probabilistic analyses to explore performance margins of natural gas infrastructure for the transport and delivery of hydrogen and hydrogen blends* [Paper presentation]. ASME 2024 Pressure Vessels and Piping Conference, Bellevue, WA.

[41] U.S. Department of Transportation, Pipeline and Hazardous Materials Safety Administration. (2024, November 18). *Pipeline safety: Identification and evaluation of potential hard spots - In-line inspection tools and analysis* (Docket No. PHMSA-2024-0176). Federal Register. https://www.govinfo.gov/content/pkg/FR-2024-11-18/pdf/2024-26725.pdf

[42] Ronevich, J., Agnani, M., Gagliano, M., Parker, J., & San Marchi, C. (2024, September 23–27). *Influence of hardness on hydrogen-assisted fracture in pipeline steels* [Paper presentation]. ASME 2024 International Pipeline Conference (IPC), Calgary, AB, Canada. https://doi.org/10.1115/IPC2024-133937

[43] Vervake, G., Bag, D., Kindel, S., Shabarchin, O., & Bolf, B. (2024, September 23–27). *An operator's experience of managing the hard spot threat* [Paper presentation]. ASME 2024 International Pipeline Conference (IPC), Calgary, AB, Canada. https://doi.org/10.1115/IPC2024-134129

[44] Ronevich, J. A., & San Marchi, C. (2021, July 13–15). *Materials compatibility concerns for hydrogen blended into natural gas* [Paper presentation]. ASME 2021 Pressure Vessels and Piping Conference, Virtual.

[45] Nishihara, Y., Inoue, N., Mori, M., & Okano, H. (2025, July 20–25). *Effect of methane-hydrogen mixed gas on fatigue crack growth characteristics of API X65 linepipe steels* [Paper presentation]. ASME 2025 Pressure Vessels and Piping Conference, Montreal, QC, Canada. https://doi.org/10.1115/PVP2025-153447

[46] Chandra, A., Thodla, R., Prewitt, T. J., Matthews, W., & Sosa, S. (2021, July 13–15). *Fatigue crack growth study of X70 line pipe steel in hydrogen containing natural gas blends* [Paper presentation]. ASME 2021 Pressure Vessels and Piping Conference, Virtual.

[47] San Marchi, C., Ronevich, J., Bortot, P., Wada, Y., Felbaum, J., & Rana, M. (2019). *Technical basis for master curve for fatigue crack growth of ferritic steels in high pressure gaseous hydrogen in ASME VIII-3 code* [Paper presentation]. ASME 2019 Pressure Vessels and Piping Conference, San Antonio, TX.